BMC Plant Biology

RESEARCH Open Access

The effect of plant growth regulators, FeO_3-CTs nanoparticles and LEDs light on the growth and biochemical compounds of black seed (*Nigella sativa* L.) callus in vitro

Ali Sobhannizadeh[1,3], Mousa Torabi Giglou[1*], Mahdi Behnamian[1], Asghar Estaji[1], Mohammad Majdi[2] and Antoni Szumny[3*]

Abstract

Background black seed (*Nigella sativa* L.) has long been utilized in traditional medicine and as a food ingredient due to its potential therapeutic properties including its effectiveness against cancer, coronaviruses, and bacterial infections. Recently, it has garnered significant attention for its rich reservoir of beneficial secondary metabolites. I*n vitro* culture of black seeds presents an efficient and modern approach for the large-scale production of these valuable compounds, offering advantages such as space efficiency, reduced time, and lower costs. This study aimed to develop and optimize a protocol for callus induction and the identification of key secondary metabolites, including thymoquinone (TQ), phenolic compounds, and flavonoids. To induce callus formation in seed explants, two plant growth regulators (PGRs) were applied individually or in combination and incorporated into Murashige and Skoog (MS) culture medium.

Results The combination of Auxin, 2,4-dichlorophenoxyacetic acid (2,4-D) and cytokinin, 6-benzylaminopurine (BAP), effectively induced callus formation in most explants, with the response varying based on concentration. The highest callus fresh weight (7.02 g) was obtained on Red(R) LED lighting with FeO_3-CTs nanoparticles (100 mg/L^{-1}), which also resulted in the highest dry weight (1.307 g) after 40 days of cultivation. Similarly, the highest levels of phenols, flavonoids and amino acids were observed under R LED with FeO_3-CTs nanoparticles (100 mg L^{-1}), while FeO_3-CTs nanoparticles at 100 and 200 mg/L^{-1}) exhibited significant effects on metabolite production. In contrast, the antioxidant activity against DPPH free radicals and total carbohydrate accumulation were enhanced in callus cultures treated with FeO_3-CTs nanoparticles (200 mg/L^{-1}) under dark conditions. Additionally, GC-MS analysis revealed that FeO_3-CTs nanoparticles (100 mg/L^{-1}) yielded the most effective enhancement of secondary metabolites under blue (B) LED light at a concentration of 295 mg/L^{-1}.

*Correspondence:
Mousa Torabi Giglou
mtorabi@uma.ac.ir
Antoni Szumny
antoni.szumny@upwr.edu.pl

Full list of author information is available at the end of the article

Conclusion The finding of this study highlights the potential of the proposed method for the large-scale production of secondary metabolites, total carbohydrates, amino acids, phenolic compounds, and flavonoids from black seed callus cultures in a controlled environment. This optimized approach offers a cost-effective and space-efficient strategy for enhancing bioactive compound synthesis, with potential applications in pharmaceutical and nutraceutical industries.

Keywords *Nigella sativa* L., Tissue culture, Stress PEG, LED, Secondary metabolite, TQ

Background

Used of herbal medicines had been as the foundation of traditional therapies throughout human history and continues to serve as a source for modern medicine. According to a report by the World Health Organization (WHO, 2020), more than three-quarters of communities in resource-limited nations rely on herbal remedies as their primary form of healthcare, as only about 60% of the population has access to conventional medicine (Sobhanizadeh et al., 2015).

Black seed (*Nigella sativa* L.) is an annual plant from the Ranunculaceae family (Ranunculaceae) and comprises a total of 22 species [105]. This plant is known under the names "Black "Cumin", "Habat Al Barke", "Tikor Azmud", "Churkoto" and "Shuniz". It is traditionally used and cultivated in the Middle East, Southern Europe, Africa and Mediterranean countries such as Iran, Pakistan, India, Turkey and Arab countries as a spice and as a natural remedy [112]. Black seeds contain essential oils (0.13–0.39%), alkaloids, sterols, phenolic compounds, saponins, fatty oils (36–50%) and proteins [90, 94]. Although it has received less attention in the scientific literature, its nutritional value is by no means low, as it contains a sufficient amount of proteins and fats and a considerable amount of essential fatty acids, amino acids, vitamins and minerals [50]. Ibn Sina (Avicenna), the famous Iranian physician of the 10th century and father of early modern medicine, described several health-promoting properties of black cumin in his famous book "The Law of Medicine", such as increasing body energy and curing fatigue and ailments [112]. Examining desiccated botanical specimens like oregano, sage, mint, and thyme, whether in their entirety or as a powdered form, are projected to drive the worldwide market to escalate from USD 5.8 billion in 2022 to USD 6.17 billion in 2023, with a Compound Annual Growth Rate (CAGR) of 6.3%. It is expected to reach 7.93 billion dollars in 2027 [97]. The global market is projected to achieve 117 billion dollars by 2029 (CAGR 7.3%) for more intricate forms like capsules, tablets, and extracts [97].

Black seed has biological and pharmacological activity such as lowering total cholesterol (TC) and triglyceride (TG) levels and blood lipids [37], lowering blood sugar levels [102], antibacterial [19], antiviral [22], improving psoriasis [53], eczema [89], acne vulgaris [100], antifungal [100], antidiabetic [41], blood pressure reduction [36], anti-arthritic [88], cleanses the liver [103], improves kidney function [13], improves the respiratory tract and lungs [111], asthma [111], coronavirus (COVID-19) [14], anti-cancer [14], anti-tumour [95], cardiotoxicity [20], oxidative stress factors decrease malondialdehyde (MDA) increase superoxide dismutase (SOD) total antioxidant capacity (TAC) [70] and increase bone strength [7] also medicinal plant can be used healing [38] and Anti-Hemorrhagic [4, 5].

The biological properties mentioned are related to the richness of various plant chemicals, mainly phenolic compounds, flavonoids, alkaloids, glycosides, terpenoids, essential oils, saponins, tannins and especially thymoquinone [11], also thymoquinone (TQ) known as the main active ingredient of the secondary metabolite (IUPAC THY 2-isopropyl-5-methylbenzo-1,4-quinone) [3]. TQ has been considered as an anti-liver cancer agent alone or in combination with other drugs [116].

Plant secondary metabolites (SMs) encompass a diverse array of small molecular weight compounds of natural origin, such as alkaloids, terpenes, glycosides, flavonoids, polyketides, essential oils, quinones, coumarins, tannins, glycosylates, cyanogenic glycosides, resins. And etc [26, 39].

The technique of seed cultivation in vitro provides a continuous source of various explants and can be used as a starting material for establishment in the culture medium when the natural growing season fails [25]. The environment is determined by many factors, the most important being the genetic structure of the plant, the composition of the environment, the size and age of the cultivated explants and the physical conditions (Uysal [105]). Metabolites derived from plants can be obtained from plants that grow in their natural environment; however, their large-scale production is restricted by various environmental and geographical limitations [114]. routines way is time-consuming as plants need several years to mature and produce the desired metabolites. An alternative ways to overcome this case used of plant tissue culture techniques to efficiently produce secondary metabolites in a short time for commercial application [52, 108]. It allows the mass propagation of plant under controlled environments, free from seasonal restrictions [72, 76].

The use of nano-technology and nano-fertilizers is increasingly being applied in agricultural crops,

particularly to enhance the understanding of their performance under laboratory cultivation conditions. Particles ranging in size from 1 to 100 nm are referred to as nanoparticles [27]. Nano fertilizers due to their special features such as the presence of nano coating for continuous release of nutrients, so small scale for better penetration, increase in surface to volume ratio and the presence of biochemical compounds to promote germination, increase plant growth, improve bioactive metabolites are used in plant tissue culture and it has turned them into a potential plant growth enhancer [24, 86, 109]. Fe chitosan-coated nano iron (CTs) is one of these elements and growth stimulus, which is a non-toxic polymer, a nitrogen-containing polysaccharide, compatible and biodegradable that is obtained from wastes of Pen squid, which is the richest source of chitin among compounds, and the skin of shrimp, crab, algae, etc [33, 113]. and due to its desirable biological properties, including biological decomposition, antimicrobial and antioxidant activity, it is used in a wide range of medical and agricultural applications, including increasing and improving production, reducing and adjusting stresses conditions like drought and etc [42, 59]. on the other hand Unfortunately, due to the low solubility of chitosan in water, the production process and practical use of its polymer is limited [58]. Moreover, compared to other biopolymers, it can be modified and used and targeted in a wide range without reducing its useful properties. Also, the impacts of several key metal oxide nanoparticles such as titanium oxide, zinc oxide, iron oxide and copper oxide have been documented for their role in enhanced production of secondary metabolites in herbals [67, 69].

The use of LED light in tissue culture has been shown to be beneficial in promoting the growth and regeneration of plant tissue and improving plant performance and health [18]. LED light has also been shown to increase the production of secondary metabolites in medicinal plants. For example, B-LED increased the amount of vanillic acid, coumaric acid and ferulic acid in Ginseng plants [78], while R-LED increased the production of lutein and glycosylates in cabbage leaves [56]. Green LED light was found to be more effective in promoting tomato growth [73]. Considering the positive effects of LED light quality on plant tissue culture and secondary metabolite production, its use is essential in the regeneration and product of secondary metabolites of plants, for vital herbal medicines in the world. LEDs have been shown to provide the light required for plant growth at a lower cost. They also have other advantages such as long lifetime, small size and volume, monochromaticity and adjustable intensity [45]. The advantages of LEDs as artificial light sources in growth chambers with controlled plant environments include high energy conversion efficiency, small volume, longer lifetime, specific wavelength, adjustable light intensity, quality and lower heat emission. The effects of LED light on different plants have been studied, and the results show that different colors of LEDs affect morphological and physiological traits in plants [57].

Plants utilize light both as an energy source for photosynthesis and as a signal to manage their growth and development. Various aspects of the light environment, such as intensity, spectrum, photoperiod, and distribution, can influence net carbon exchange rates (NCRE), morphology, and yield. LED arrays with adjustable spectra enable programmable control of the light environmental and can be directly installed in the boxes to enhance light distribution. In addition, nanoparticles are readily available to the plant and can be used as a stimulus for the production and propagation of secondary metabolites. Therefore, the effect of intensity, spectrum and FeO_3-CTs-NPs on black seed callus (*Nigella sativa*) were investigated in controlled environment systems (CES) and in vitro (tissue culture) Also, parameters like phenolic and flavonoid compounds, antioxidant activity, and GC-MS analysis and so on were evaluated.

Results

Synthesis and characterization Fe-CTs NPs

FT-IR spectral analysis of chitosan revealed absorption peaks at 3447 cm^{-1} corresponding to amide functional groups and O-H bonds associated with adsorbed water molecules [33, 47]. In the magnetic chitosan/Fe_3O4 composite, characteristic peaks at 3447, 2924, and 1630 cm^{-1} indicated the presence of chitosan, showing slight shifts compared to pure chitosan. The peak at 590 cm^{-1} confirmed the Fe-O bond, substantiating the presence of Fe_3O_4 magnetic nanoparticles within the structure [75]. The XRD spectrum in (Fig. 1a) displayed peaks at $2\theta = 30.3°$, 35.7°, 43.3°, 53.8°, 57.3°, and 63° corresponding to (220), (311), (400), (422), (511), and (440) plates of Fe_3O4 NPs confirming their crystalline structure [12]. The shape and morphology of magnetic chitosan nanoparticles were investigated using SEM and TEM. The SEM picture in (Fig. 1b) indicates a spherical shape with particle sizes ranging from 50 to 100 nm. Furthermore, the TEM image confirmed the morphology of the NPs and their size, which was approximately (10–20) nm. Accumulation of NPs can also be observed [40].

Callus induction and multiplication

To induce callus formation, sterilized black seed seeds were cultivated in MS medium with 2,4-D and BAP. Mancozeb (100 mg L^{-1}) effectively reduced fungal contamination. MS medium, with the right PGRs, is commonly used for callus formation [16, 49]. Callus initiation success depended on disinfection, PGR composition, and their interactions. Explants showed higher browning in BAP-treated media, but better viability with 2,4-D. The

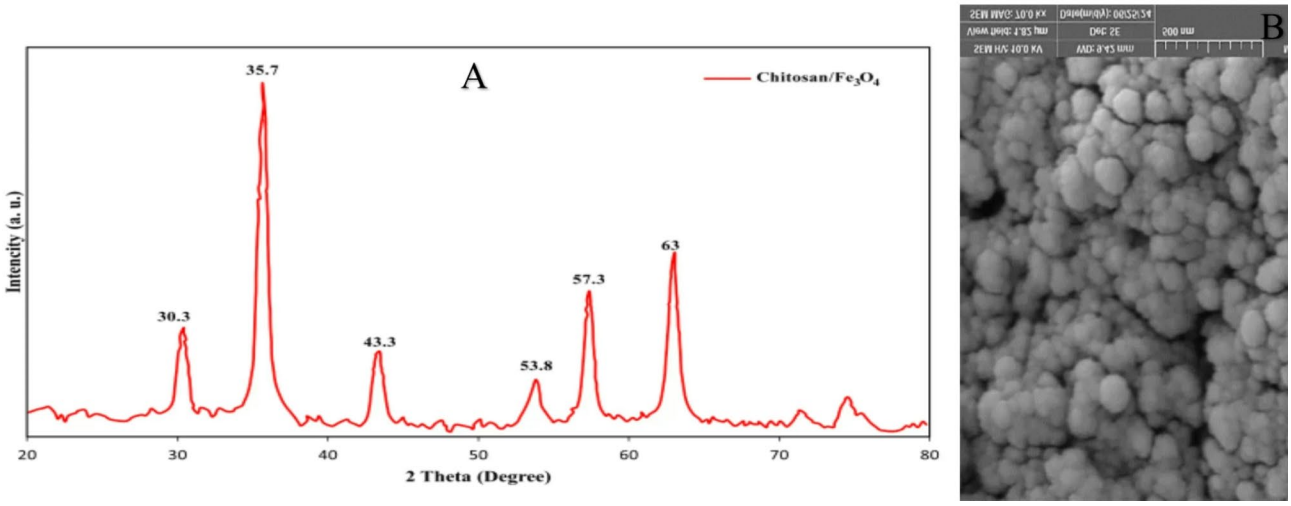

Fig. 1 XRD (**A**) and SEM (**B**), analyses of starting material and Feo_3-CT_S NPs

highest viability occurred with 2 mg L^{-1} 2,4-D + 0.5 or 1 mg L^{-1} BAP.

Callus initiation in black seed took 13–16 days, similar to other species (Giglou, Giglou, Estaji, et al., [35]; Rajila & Arunprasath [82, 96]. Callus induction was highest with 2 mg L^{-1} 2,4-D, followed by 1 mg L^{-1} 2,4-D. BAP improved callus formation, especially at a 2:1 or 1:0.5 auxin-to-cytokinin ratio, but the best results were with 2 mg L^{-1} 2,4-D without BAP. Similar findings were reported in other plants [6, 46, 60].

Based on high callus formation rates, size, fresh/dry weight, four optimized culture conditions were identified for black seed callus propagation:. MS medium supplemented with (1 + 0.5 mg L^{-1} BAP and 2,4-D), (1 + 2 mg L^{-1} BAP and 2,4-D), and MS solid medium with 1 or 2 mg L^{-1} 2,4-D alone. The final experimental setup was conducted using 1 + 2 mg L^{-1} BAP and 2,4-D as the optimal combination. The best culture conditions for black seed callus were MS medium with 1 + 0.5 mg L^{-1}, 1 + 2 mg L^{-1} BAP and 2,4-D, or 1–2 mg L^{-1} 2,4-D alone. The optimal combination was 1 + 2 mg L^{-1} BAP and 2,4-D (Fig. 2).

Yield callus

The results of this study indicate that fresh weight (FW) and dry weight (DW) of callus increase significantly under LED-colored light and FeO_3-CTs-NPs treatments compared to normal conditions. The most notable weight changes were observed in explants exposed to R LED combined with FeO_3-CTs NPs (100 mg L^{-1}). Specifically, this treatment led to a significant increase in callus volume and weight (7.02 g), whereas the lowest weight was recorded under W LED control conditions (2.81 g) (Figs. 3 and 4).

The highest callus weight were recorded in the R LED Box and FeO_3-CTs nanoparticles at concentrations of 50 mg L^{-1} liter (6.81 g) and 100 mg L^{-1} liter(7.02 g). In contrast, the lowest weight(2.81 g) observed in the W LED control treatment. The results indicated a gradual increase in callus weight during the first 21 days across all media. Within seven days, callus weight increased by several grams in different culture conditions. Notably, fresh weights in theR LED and FeO_3-CT nanoparticles (50 and 100 mg L^{-1}) treatments as well as in the B LED and FeO_3-CT nanoparticles (50 and 100 mg L^{-1}) treatments, showed a significant increase from the third week to the end of the fourth week (Fig. 4 and 5).

Wet weight and callus size were measured weekly over a 35-days period. The results showed a significant difference in fresh callus weight after 21 days of cultivation, with the R LED and FeO_3-CTs nanoparticle (100 mg L^{-1}) treatment yielding the highest weight among all conditions. In the 35-day culture, the fresh weight of callus in the R LED and FeO_3-CTs nanoparticle (100 mg L^{-1}) treatment remained the highest compared to other treatments. Specifically, the fresh callus weight under these conditions was 4.6 g at 21 days, 6.1 g at 28 days, and 7.02 g at 35 days. After 35 days, the difference between R LED with FeO_3-CTs nanoparticles (50 and 100 mg L^{-1}) and other treatments was statistically significant. The lowest and highest fresh callus weights recorded during the 35-day period were 2.81 g and 7.02 g, respectively, showing a significant variation among different culture conditions.

Callus size and volume changes were assessed by measuring the callus area in square centimeters (cm^2). From the middle of the third week until the end of the cultivation period, callus size in the R LED treatment with FeO_3-CTs nanoparticles (50 and 100 mg L^{-1}) was visibly larger than in other media. The highest increase in callus area (10.13 cm^2) was observed in the R LED culture medium with FeO_3-CTs nanoparticles (100 mg L^{-1}) over 35 days,

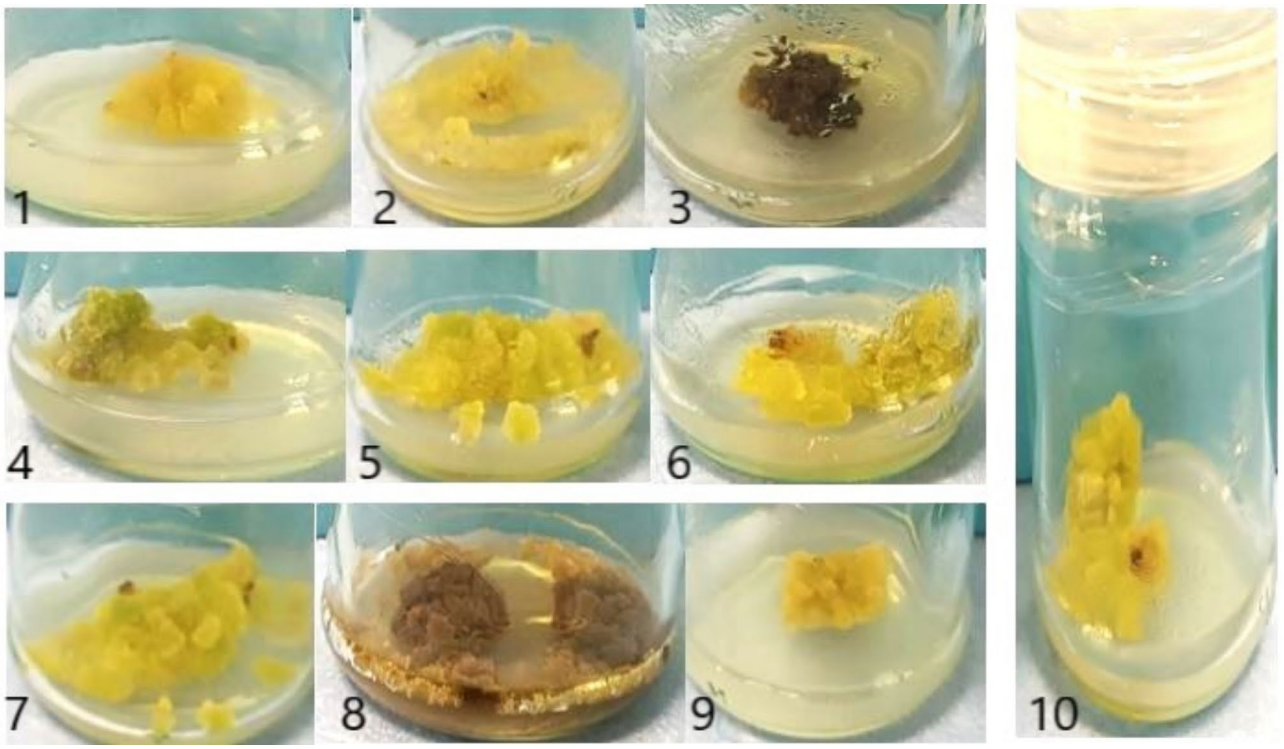

Fig. 2 The treatment of 2,4-D and BAP for callus formation rate. 2,4-D and BAP 1- (1 + 0.5 mg L^{-1}), 2- (1 + 1 mg L^{-1}), 3- (1 + 2 mg L^{-1}), 4- (2 + 0.5 mg L^{-1}), 5- (2 + 1 mg L^{-1}), 6- (2 + 2 mg L^{-1}), 7- (4 + 0.5 mg L^{-1}), 8- (4 + 1 mg L^{-1}), 9- (4 + 2 mg L^{-1}), 10- (2 + 0 mg L^{-1})

compared to 9.64 cm^2 in other treatments (Fig. 3). After 35 days, the maximum callus size increase in R LED with FeO_3-CTs nanoparticles (50 and 100 mg L^{-1}) and B LED with FeO_3-CTs nanoparticles (50 and 100 mg L^{-1}) was recorded at 9.64, 10.13, 9.16, and 8.93 cm^2, respectively. In contrast, the control callus in dark and W LED conditions exhibited smaller sizes, measuring 6.14 cm^2 and 6.51 cm^2, respectively. These results indicate a correlation between callus weight, size, and optimal media for callus propagation. The R LED medium with FeO_3-CTs nanoparticles (100 mg L^{-1}) is recommended for Nigella sativa callus proliferation, as it enhances cellular activity, promotes cell division, and results in a larger, more voluminous callus with the highest fresh weight.

DPPH and quercetin (QE)

In this study, the antioxidant activity of the callus extracts was evaluated using the DPPH ways to determine the effact of different types and concentrations of PGRs. DPPH is a stable free radical and is a widely used method for measuring the antioxidant potential of various compounds. This method offers several advantages, including simplicity, rapid execution, high accuracy, reliability, and the lack of need for complex instrumentation [93]. A significant difference in DPPH antioxidant activity was observed among callii in different treatments. The highest and lowest antioxidant activity were recorded in W LED and R LED treatments, at 51.25% and 38.11%, respectively. Additionally, FeO_3-CTs nanoparticles at concentrations of 100 and 200 mg L^{-1} exhibited high antioxidant activity, measuring 50.58% and 50.80%, respectively, while the lowest activity (39.60%) was observed with FeO_3-CTs nanoparticles at 50 mg L^{-1} (Table 1).

Although the DPPH assay provides high accuracy in detecting minor variations in antioxidant activity, its limitation lies in its solubility in polar matrices, which can sometimes result in slow reactions between DPPH and antioxidants [61]. Minor differences in antioxidant capacity were observed between LED light and nanoparticles in a medium of similar media composition (2,4-D medium and BAP 1 + 2 mg L^{-1}). Our findings support the use of in vitro black seed cultures, as the DPPH assay demonstrated a strong antioxidant response in these cultures.

The effect of LED radiation and nanoparticles was measured over a of 35-days period, revealing no significant difference in quercetin content among the callus of the seed explants. However, the individual treatments with FeO_3-CTs nanoparticles at concentrations of 100 and 200 mg L^{-1} showed significant effects, with quercetin levels of 3.31 mg/g and 3.30 mg/g, respectively (Table 1).

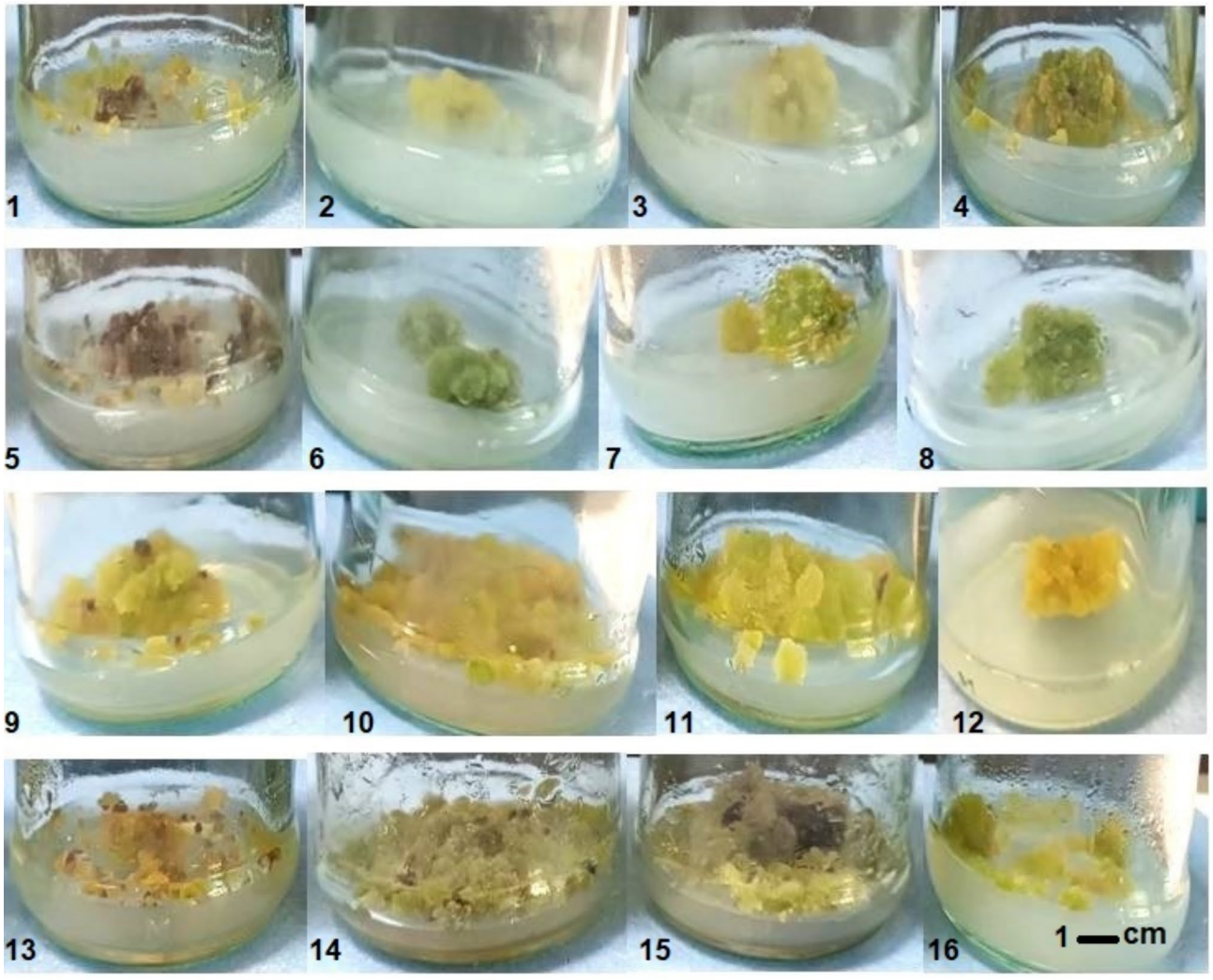

Fig. 3 Changes in growth and callus size (cm^2) at LEDs and FeO_3-CTs Nanoparticles. D LED, FeO_3-CTs nanoparticles (0, 50, 100 and 200 mg L^{-1}) (1, 2, 3, 4) respectively, W LED, FeO_3-CTs nanoparticles (0, 50, 100 and 200 mg L^{-1}) (5, 6, 7, 8), R LED, FeO_3-CTs nanoparticles (0, 50, 100 and 200 mg L^{-1}) (9, 10, 11, 12), B LED, FeO_3-CTs nanoparticles (0, 50, 100 and 200 mg L^{-1}) (13, 14, 15, 16)

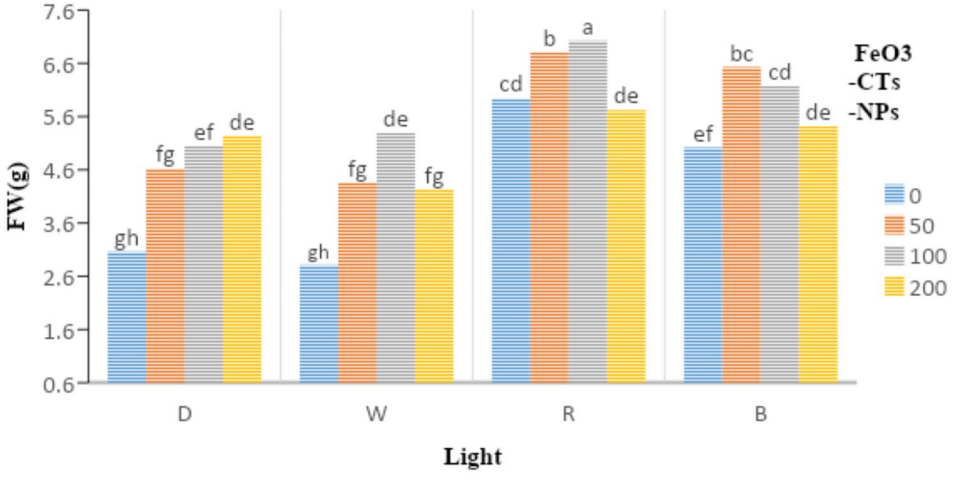

Fig. 4 Fresh weight (g) in callus black seed with LED and nano particle condition

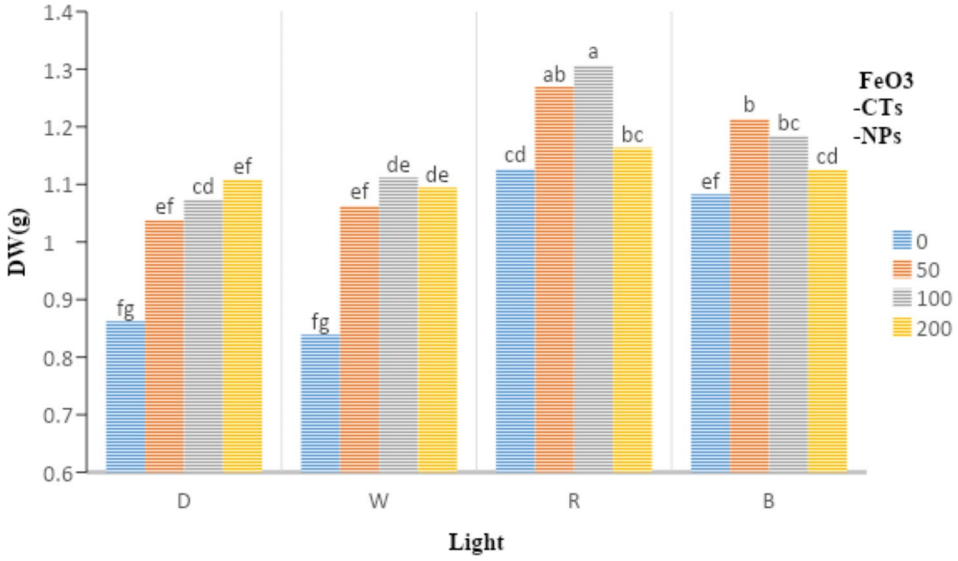

Fig. 5 Dry weight (g) in callus black seed with LED and nano particle condition

Table 1 Changes in the DPPH and QE with difference LED and nano particle condition

Light	NANO	DPPH	QE
D		43.862 bc	-
W		51.254 a	-
R		38.11 cd	-
B		48.80 ab	-
	0	41.433 b	2.81 b
	50	39.60 bc	3.15 ab
	100	50.58 a	3.31 a
	200	50.80 a	3.30 a
ANOVA			
LIGHT		*	ns
NANO		*	*
LIGHT*NANO		ns	ns

* Significant at 5% level, ** Significant at 1% probability level, ns No Significant difference

Total carbohydrate (TC) content

The results indicate that the total carbohydrate content under control conditions and B LED, as well as with FeO_3-CTs nanoparticles at 200 mg L^{-1} was significantly higher compared to other LED and FeO_3-CTs nanoparticle treatments.

Figure 6 illustrates the effect of different LED treatments and nanoparticle concentrations on the total carbohydrate and starch content of *Nigella sativa* callus after 35 days of growth. Overall, the total carbohydrate content in callus increased in parallel with the rise in FeO_3-CTs nanoparticle concentration (200 mg L^{-1}), particularly under dark conditions, compared to the control and ther LED treatment. The highest carbohydrate accumulation was observed at 200 mg L^{-1} FeO_3-CTs nanoparticles under dark conditions (1.93 mg L^{-1}), significantly higher than the control (1.07 mg L^{-1}). In contrast, lower

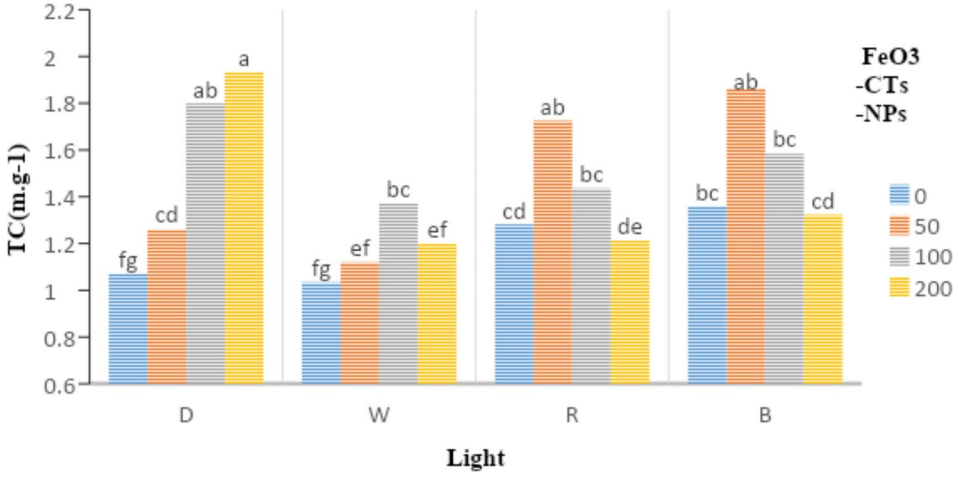

Fig. 6 Total Carbohydrate (TC) ($m.g^{-1}$) content in callus black seed with LED and Nano particle condition

FeO_3-CTs nanoparticle concentrations (50 mg L^{-1}) in B and R LED treatments individually led to an increase in total carbohydrate content (1.86 and 1.79 mg L^{-1}, respectively). However, applying FeO_3-CT nanoparticles at a high concentration (200 mg L^{-1}) under LED lighting resulted in a reduction in total carbohydrate content, particularly under W LED (1.19 mg L^{-1}). Moreover, the combination of FeO_3-CTs nanoparticles at higher concentrations with LED treatments generally reduced total carbohydrate content compared to the dark box.

Total phenolic (TPC) and flavonoids (TFC) content

The phenolic content of the callus extract was estimated by spectrophotometry at 750 nm using gallic acid as a reference. The combination of hormonal treatments and LED lighting significantly impacted the phenolic content of Nigella sativa callus across different media. The highest accumulation of TPC and TFC was observed under R LED and FeO_3-CTs nanoparticles 100 (mg L^{-1}), with values ranging from 48.67 to 22.99 mg L^{-1}. The lowest phenolic content was recorded in the control treatment, while the highest (48.67 mg L^{-1}) was found in the medium supplemented with R LED and 100 mg L^{-1} FeO_3-CTs nanoparticles. Additionally, significant differences in total phenolic content were observed among different LED treatments. The highest phenolic accumulation was detected in R LED, B LED and FeO_3-CTs nanoparticle treatments (50, 100 and 200 mg L^{-1}), with recorded values of 48.67, 45.63 and 41.58 mg L^{-1}, respectively. These findings highlight the role of LED type and FeO_3-CTs nanoparticle concentration in enhancing the phenolic content of black seed callus (Fig. 7).

The total flavonoid content in the callus extract was estimated using a spectrophotometric method at a wavelength of 510 nm, with catechin as the reference standard. The highest flavonoid accumulation was observed in R, B LED media combined with FeO_3-CTs nanoparticles (50 and 100 mg L^{-1}), recording values of 27.88, 25.88 and 24.39 mg L^{-1}, respectively. Furthermore, the results indicate that the other LED treatments did not exhibit significant difference in flavonoid content. The flavonoid levels ranged from 18.18 to 18.60 mg L^{-1} in W LED and dark conditions when combined with FeO_3-CTs nanoparticles (50 and 200 mg L^{-1}) (Fig. 8).

The results obtained demonstrated that the use of LED light and FeO_3-CTs nanoparticles individually promotes approximately similar amounts of phenolic compounds. However, the combination of R LED treatment with FeO_3-CTs nanoparticles (100 mg L^{-1}) led to a significantly higher phenolic content. Additionally, flavonoid content increased under R and B LED with FeO_3-CTs nanoparticles (50 and 100 mg L^{-1}) compared to the other LED treatments. Thus, the combination of R and B LEDs with FeO_3-CTs nanoparticles (50 and 100 mg L^{-1}) in the propagation medium for black seed callus was preferred for enhanced flavonoid production. Lower and moderate concentrations of nanoparticles, particularly when combined with R-LED, were found to stimulate greater production of phenolics and flavonoids, highlighting the essential role of light and nanoparticles in metabolic regulation within black seed callus cultures. All callus cultures shared the same composition, except for variations in light treatments and nanoparticle applications. Ultimately, it was determined that the combination of R LED and FeO_3-CTs nanoparticles (100 mg L^{-1}) yielded the highest levels of phenols and flavonoids incallus cultures. Moreover, these results confirmed that the using 2,4-D (1 mg L^{-1}) and BAP (2 mg L^{-1}) in the Black seed callus culture medium for resulted in higher phenolics and flavonoid levels compared to other PGR concentrations of PGRs examined in this study.

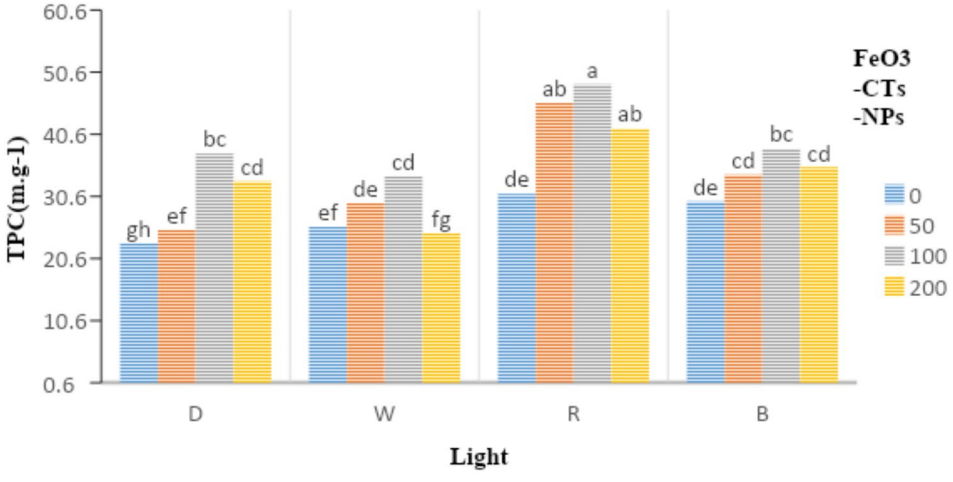

Fig. 7 Total phenol (TPC) ($m.g^{-1}$) content in callus black seed with LED and Nanoparticle condition

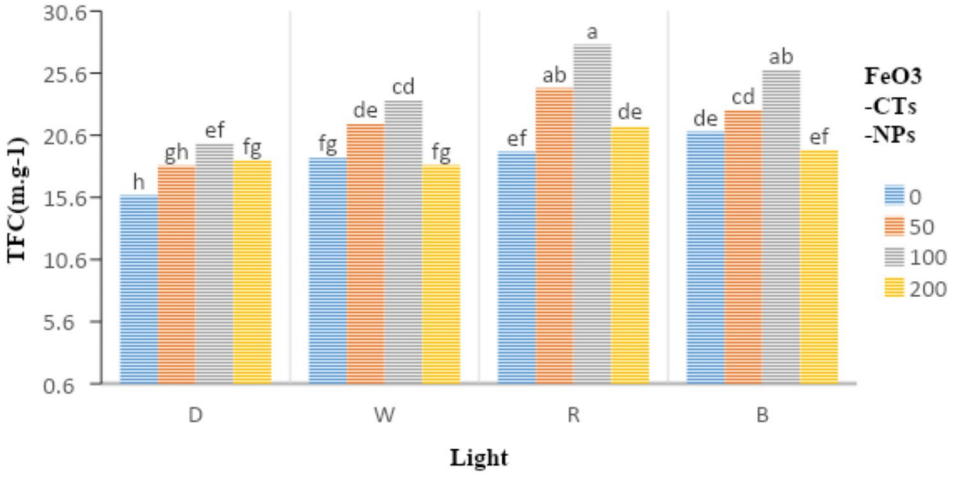

Fig. 8 Flavonoids (TFC) (m.g^{-1}) content in callus black seed with LED and Nano particle condition

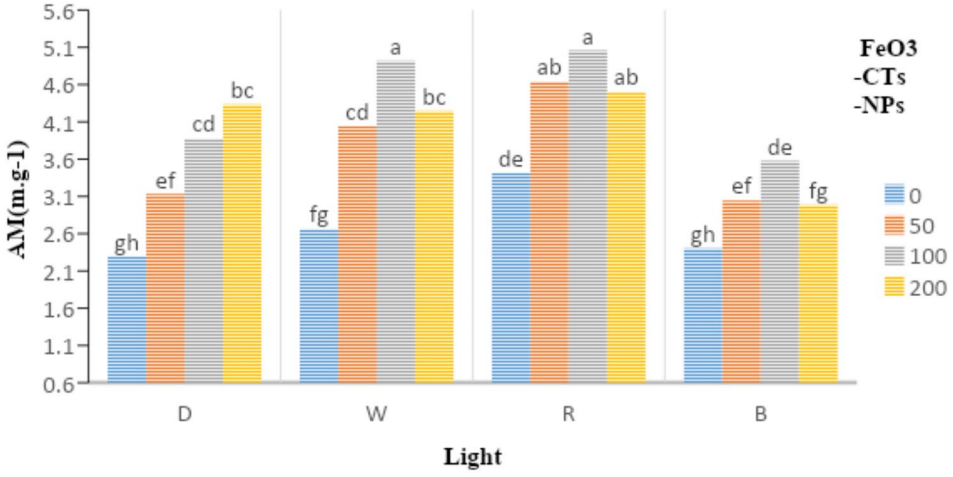

Fig. 9 Amino Acid (AM) (m.g^{-1}) in callus black seed with LED and Nano particle condition

Total amino acid content (TAMc)

In the study, total amino acids content (TAMc) exhibited an increasing trend in R and W LEDs light treatments in combination with nanoparticle FeO_3-CTs nanoparticles at concentrations of 50, 100 and 200 mg L^{-1}. Notably, TAMc levels rose with increasing nanoparticle concentrations, peaking at 100 mg L^{-1} under R and W LED conditions. Additionally a significant increase in TAMc concentration was observed in the dark treatment compared to the control. Among the tested light conditions, light conditions, R and W LED treatments had the most pronounced effect on TAMc accumulation, with the highest values recorded at 5.05 and 4.91 mg L^{-1} respectively, when FeO_3-CTs nanoparticles were applied at 100 mg L^{-1}. In contrast, the lowest TAMc content (2.3 mg L^{-1}) was observed on the Dark contorol condition without nanoparticles. As expected, intermediates of central metabolism, primarily amino and organic acids, were found in significantly higher concentrations in callus tissues exposed to R and W LED with 100 mg L^{-1} FeO_3-CTs nanoparticles compared to B LED treatments with varying nanoparticle concentrations (Fig. 9).

The amount of thymoquinone (TQ) in callus

According to the results, the GC-MS analysis of the methanolic extract of callus revealed that Thymoquinone (TQ) content ranged from 295 to 120 mg^{-1}. The highest TQ concentration (295 mg L^{-1}) was observed under B LED treatment with FeO_3-CTs nanoparticles (100 mg L^{-1}), while the lowest (120 mg L^{-1}) was recorded under W LED control conditions (Fig. 10).

Correlation matrix

In examining the results of the correlation, it was observed that there is a positive and negative correlation between the traits investigated in this research, wich illustrated in heatmap.

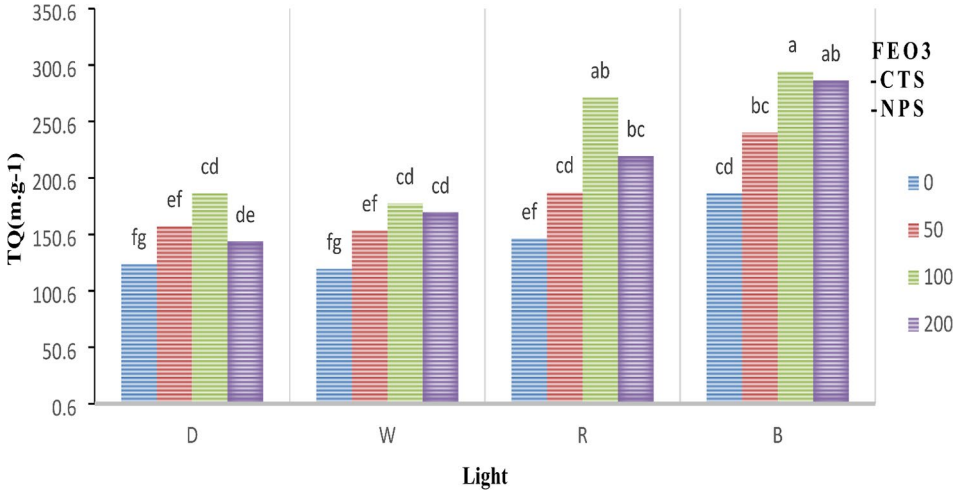

Fig. 10 Thymoquinone (TQ) (m.g^{-1}) in callus black seed with LED and Nano particle condition

The results showed that the highest correlation there were between TQ with DW and QE. Also, the correlation between TFC and TC and TPC were in highest level, the results of this research showed that there is a negative correlation between TC and TQ and AM, and increase in TC caused a decrease in TQ and AM in callus. In the correlation between DPPH and FW, it was observed that they have a reverse relationship between these two traits (Fig. 11).

Discussion

A plant cell retains its totipotency in culture, allowing it to synthesize compounds found in the original plant [28]. Disorganized proliferation occurs as a result of the wound healing cascade, which, along with the initiation of cellular mitosis, begins at the outer layer of the freshly sectioned explant. In in vitro, callus formation occurs through disorganized growth as a result of the wound healing process, along with the initiation of cellular mitosis, which begins at the outer layer of the recently sectioned explant after being placed in growth-promoting conditions [29]. The callus generated through dedifferentiation consists mainly of unorganized parenchymatous cells. Additionally, callus proliferations influenced by gravity and variations in light intensity, which induce polarization [77]. In this study, the use of different concentrations of auxin combined with cytokinin significantly affected callus productivity. However, high concentration of 2,4-D alone led to competition, potentially altering auxin's role in promoting cell division. Auxins are essential for initiating callus growth, and their concentration directly influences callus fresh weight and volume [81, 110].

There is a strong correlation between callus induction efficiency and the combination of medium and treatment (LEDs, FeO3-CTs nanoparticles), particularly plant growth regulators (PGRs) like auxin and cytokinin. These PGRs play a crucial role in callus culture, as they regulate key plant processes such as cell division, elongation, and morphogenesis [122]. Cytokinin alone does not effect parenchyma cell growth. However, when auxin is present without cytokinin, cells enlarge but do not divide. However, when cytokinin and auxin are added together, cells grow and differentiate. An equal ratio of cytokinin and auxin results in an undifferentiated callus, whereas a higher cytokinin concentration promotes shoot bud formation, and a higher auxin concentration stimulates root development [8, 15, 68]. Furthermore, the type of explant used significantly impacts callus formation. For example, in a study on *Lycium barbarum* microspecies, hypocotyl explants formed more callus compared to root and leaf explants [106]. Growth hormones have a positive correlation with the rate of callus proliferation, with auxin playing a particularly crucial role in this process [115]. The findings of this study align with those of Sobhanizadeh [98]. Specifically, an investigation into the effects of growth stimulants on callus formation revealed that the combination of 2,4-D and BAP significantly enhanced the fresh weight of black seed callus. This increase was approximately seven times greater than that observed with other PGR treatments applied to root explants of Cnidium officinale [1]. The role of quercetin and DPPH in defending against light and nanoparticle-induced stress has been widely reported [43]. These compounds exhibit strong antioxidant activity due to their structural composition, where a higher number of hydroxyl groups and double bonds enhance their antioxidative potential [64]. Under stress conditions, the flavonoid 3'-hydroxylase enzyme which ultimately serves as a precursor for quercetin biosynthesis [87, 120]. The use of these light qualities allows researchers to study the distinct roles of photoreceptors (e.g., phytochromes for RL and

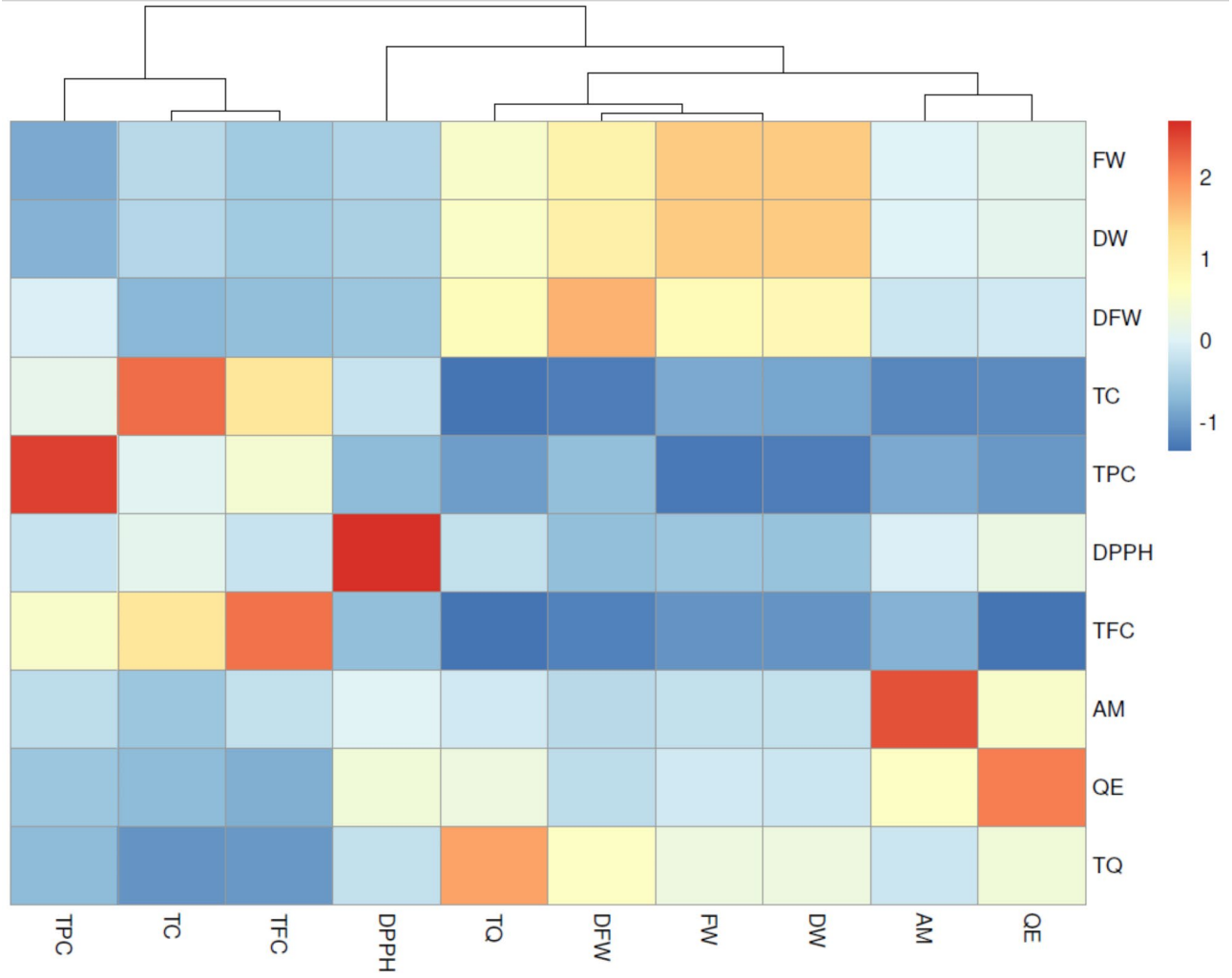

Fig. 11 The heat map of pearson correlation analysis representing the positive, negative or inconsequential relationships among the studies traits in callus

cryptochromes for BL) in regulating callus growth, oxidative stress, and gene expression, providing insights into light-mediated stress responses and signaling pathways [124]; Pashkovskiy et al. 2017; Yue et al. [114].

In this study, prolonged exposure to FeO_3 nanoparticles at higher concentrations (100 and 200 mg L^{-1}) over five-weeks was found to stimulate quercetin biosynthesis, enhancing antioxidant capacity. On the other hand, quercetin accumulation did not significantly differ under various LED photoperiod treatments, suggesting that the biosynthetic pathway may prioritize the accumulation of dihydrokaempferol, thereby mitigating cell damage. LED light is known to regulate photosynthesis and various enzymes involved in phenolic compound synthesis [71, 85]. The activity of key enzymes in the phenylpropanoid and shikimic acid pathways, along with gene expression patterns, may further explain metabolic changes in callus cultures. Terpenoid pathway, also known as the isoprenoid pathway, consists of two distinct biosynthetic routes in plants: the mevalonic acid (MVA) pathway and the methyl-D-erythritol (MEP) Pathway. The MVA pathway serves as a precursor for the synthesis of triterpenoids and polyphenols [32, 107]. Research on plant tissue cultures has led to the production of various bioactive molecules in large quantities for therapeutic purposes. One of the most important precious origins for conventional pharmaceutical, medicine, food, and cosmetic industries are plant secondary metabolites [83].

Phenolic compounds possess crucial biological properties, including antioxidant, anti-inflammatory, and anticancer activities [64]. For instance, gallic acid exhibits pharmacological and cosmetic benefits by restoring epidermal barrier function, addressing damage from conditions such as Crohn's disease (NCBI, 2022). Meanwhile, flavonoids like quercetin are in high demand due to their extensive biotechnological applications [9]. Quercetin has been explored as an antioxidant in cancer therapy due to its selective toxicity toward cancer cells [55, 91]. Several

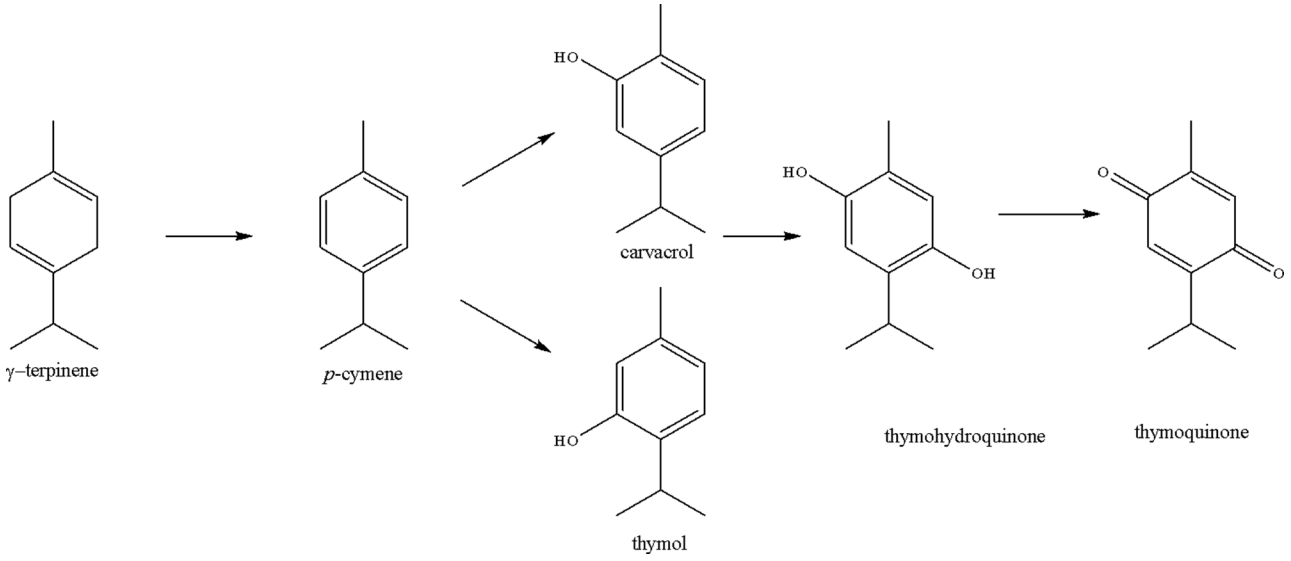

Fig. 12 Synthetic preparation of TQ based pharmaceuticals [21, 98]

studies have demonstrated that the growth of medicinal plants under stress conditions —such as exposure to nanoparticles and LED lighting—induces morphological, physiological, and biochemical modifications, affecting the biosynthesis of key secondary metabolites (Heydarnajad et al., 2025; Narayani & Srivastava [74]. One of the most significant environmental tension affecting plants is the exposure to different light emitting diodes (LEDs) and nanoparticles, leading to notable impacts on the biosynthesis of defense-related secondary metabolites [80, 101].Recent research by Giglou et al. [34] reported that the application of FeO3-CT nanoparticles at higher concentrations under dark conditions significantly increased total carbohydrate content. Similarly, LED treatments also resulted in a substantial elevation of carbohydrate levels compared to control conditions, aligning with the findings of the present study (Giglou, Giglou, Esmaeilpour, et al., [34]).The cultivation of plant cells and organs provides a sustainable, controllable and environmentally friendly tool for the industrial production of natural plant resources [76]. Over the last decade, lot of investigations on callus and cell suspension cultivation have been issued in an intention to evolve alternate origins of phenolic and flavonoid composites like *Clinacanthus nutans* [17], *Thevetia peruviana* [63], *Gymnosporia buxifolia* [54] and *Nigella sativa* [99]. In an exploration for the product of phenolic composites in the herbal *Zingiber officinale Rosc* in vitro conditions, it showed that the phenolic composites of the callus in vitro were significantly advanced than the cultivated plant [10]. Similarly, a comparative study of three Opuntia species revealed that laboratory-grown Opuntia strep acantha demonstrated higher antioxidant activity and polyphenol content than the other species tested [84].

In the natural biosynthetic pathway of thymoquinone (TQ), a crucial gene known as *geranyl diphosphate synthase* (GPPS) plays a key role in the production of quinones and phenols in medicinal plants. The proposed biosynthetic pathway for quinone and phenol synthesis is illustrated in Fig. 12. Geranyl diphosphate (GPP) serves as the precursor for this cycle, leading to the formation of γ-terpinene (a phenol), which subsequently converts into p-cymene and carvacrol, ultimately resulting in the synthesis of TQ [51, 123].

Thymoquinone is primarily extracted from various plant sources including the seeds of *N. sativa.* The presence of this combination has already been verified in kinds of the *Lamiaceae* tribe like as *Agastache*, *Coridothymus*, *Monarda*, *Mosla*, *Origanum*, *Satureja*, *Thymbra* and *Thymus*. It has existed establish in the class *Tetraclinis*, *Cupressus* and *Juniperus* from the family Cupressaceae [30]. total origins of TQ are supposed to own a monophyletic root in the magnolia order (*Magnolioideae*), however changeable in another categories [2]. One major natural source of TQ is oregano (*Origanum* spp.), particularly *O. vulgare*, *O. minutiflorum*, and *O. schwarz*, as well as thyme (*Thymus vulgaris*), *N. sativa*, and other aromatic plant extracts. The concentration of aromatic thymoquinone in these extracts must be at least 70% of the total dry weight (DW) to meet commercial and medicinal standards (Alu'datt et al., 2023; Etheve et al., [23]. Also Thymoquinone (TQ) exhibits anticancer properties by inhibiting breast cancer cell growth, inducing apoptosis, and modulating signaling pathways like NF-κB and PI3K, with studies exploring its pharmacokinetics, combination therapies, and drug delivery systems [117, 125].

In this study, we developed an optimized and effective method for producing Nigella sativa (black seed) callus to enhance the extraction of phenols, flavonoids, and other secondary metabolites. The culture media were carefully optimized by adjusting plant growth regulators (PGRs), LED light conditions, and FeO_3-CTs nanoparticle concentrations to maximize biomass, metabolite yield, and polyphenol content. The most effective medium for increasing biomass and callus size was MS medium supplemented with 2 mg L^{-1} 2,4-D and 1 mg L^{-1} BAP, combined with red (R) LED light and FeO_3-CTs nanoparticles (50 and 100 mg L^{-1}). Additionally, the combination of 2,4-D + BAP (2 + 1 mg L^{-1}) with blue (B) and red (R) LEDs and FeO_3-CTs nanoparticles (50 and 100 mg L^{-1}) was the most effective for accumulating volatile metabolites.

Due to their atypical shape, measuring the actual size of the callus provides more accurate consequence in measuring the diameter of the calli, as does the spectrophotometric measurement of the secondary metabolite content in black seed callus obtained from different combinations of LED and FeO_3-CT nanoparticles. The results of this test showed that the amount of TPC, TFC and AC is significantly affected by LED and FeO_3-CTs nanoparticles. On the other hand, the medium containing 2,4-D + BAP (2 + 1 mg L^{-1}) in the dark chamber with FeO_3-CTs nanoparticles (200 mg L-1) was the best for higher biomass and total carbohydrate accumulation.

Additionally, callus extracts obtained from MS medium containing 2 mg L^{-1} 2,4-D + 1 mg L^{-1} BAP under red and blue LED conditions with FeO_3-CTs nanoparticles (50 and 100 mg L^{-1}) present a promising new approach for synthesizing secondary metabolites. The antioxidant profile of these cultures exhibited high levels of total phenolic compounds, polyphenols, and flavonoids, supporting their potential applications. Given these promising results, further laboratory tests are recommended to validate and optimize the herbal parameters examined in this study. Overall, our findings pave the way for large-scale production of Nigella sativa secondary metabolites, particularly thymoquinone, for pharmaceutical and industrial applications.

Due to the irregular shape of the callus, direct size measurements provided more accurate results than diameter-based measurements, while spectrophotometric analysis effectively quantified secondary metabolites in black seed callus grown under different LED and nanoparticle conditions. The results demonstrated that total phenolic content (TPC), total flavonoid content (TFC), and antioxidant capacity (AC) were significantly influenced by both LED light and FeO_3-CTs nanoparticles. The highest biomass and total carbohydrate accumulation were achieved in cultures grown in the dark with FeO_3-CTs nanoparticles (200 mg L^{-1}). Furthermore, MS medium supplemented with 2 + 1 mg L^{-1} 2,4-D + BAP, in white (W) and red (R) LED conditions with FeO_3-CTs nanoparticles (100 mg L^{-1}), was most effective for enhancing amino acid production.

Conclusion

The results of this study indicate that a medium with a high auxin content is preferable for in vitro studies on clonal propagation of black cumin plants if the aim is callus formation. This finding is consistent with previous research, which has shown that auxins, such as 2,4-D, play a significant role in promoting cell division and dedifferentiation, key processes in callus formation [8]. However, for direct shoot regeneration, a medium containing BAP or another cytokinin is preferred. Cytokinins are essential for promoting cell differentiation and shoot organogenesis, and their application in combination with auxins has been widely reported to induce regenerative pathways [68]. The use of cytokinin-rich media facilitates the development of shoot buds from the callus, contributing to successful clonal propagation in plant tissue culture [15].

For the production of thymoquinone (TQ) and other secondary metabolites, the most effective stimulation combination was the use of blue (B) and red (R) LED light with FeO3-CTs nanoparticles at a concentration of 100 mg L^{-1}. This result is in line with previous studies demonstrating that LED light spectra can significantly influence plant growth and the production of secondary metabolites, particularly flavonoids and terpenoids [71, 85]. LEDs, especially blue and red light, are known to enhance photosynthesis and regulate the synthesis of phenolic compounds by modulating various enzymatic activities in plants. The use of FeO3-CTs nanoparticles in combination with LED light further improved the yield of thymoquinone and other secondary metabolites, likely due to the synergistic effects of nanoparticles in enhancing nutrient uptake and stimulating antioxidant enzyme activity [34].

Furthermore, we observed that the combination of different LED light conditions, such as D, W, R, and B, with FeO3-CTs nanoparticles (50 and 100 mg L^{-1}), yielded favorable results for enhancing the production of other valuable compounds. These combinations promoted antioxidant activity and significantly impacted the synthesis of polyphenols, flavonoids, and other bioactive molecules, which have therapeutic applications in medicine and cosmetics. This highlights the importance of optimizing both light conditions and nanoparticle concentrations to maximize the production of medicinally valuable compounds in vitro. Future studies should aim to explore the interactions between different LED light spectra and nanoparticle types to further optimize secondary metabolite production, particularly focusing on

the long-term effects of these treatments on plant health and yield.

Additionally, to optimize the production of bioactive compounds, future research should explore the optimal ratio of red and blue light (RL: BL) or variations in light intensity to further enhance callus growth and secondary metabolite production, focusing particularly on antioxidant activity and gene expression (e.g., RbohD, POR B/C). Studies have shown that the balance between red and blue light affects plant morphology and secondary metabolite biosynthesis, potentially providing a more efficient strategy for large-scale production of bioactive compounds. Additionally, the impact of light intensity on metabolic pathways involved in the synthesis of antioxidants, flavonoids, and terpenoids needs to be further investigated, as light is a critical factor in plant metabolic regulation.

This approach could improve industrial-scale bioactive compound yields. The development of scalable systems for the production of bioactive compounds using tissue culture, LED lights, and nanoparticles holds promise for the pharmaceutical and cosmetic industries. The ability to produce high-quality, bioactive compounds in controlled in vitro systems is crucial for reducing reliance on wild plant populations and ensuring a sustainable supply of valuable secondary metabolites.

Furthermore, investigating different nanoparticle types and their effects on secondary metabolite production would offer promising avenues for future studies, as well as applying this protocol to other medicinal plants for broader applicability. Nanoparticles, such as iron oxide (FeO3-CTs), have been shown to enhance the production of secondary metabolites by interacting with plant cells and promoting cellular responses that favor biosynthesis (Zhao et al., 2022). Exploring other types of nanoparticles, such as zinc oxide or silver, and their interactions with different plant species could provide valuable insights into optimizing secondary metabolite production. Additionally, applying this protocol to other medicinal plants could expand its applicability, allowing for the mass production of a wide range of bioactive compounds for various industrial applications.

In conclusion, the integration of FeO3-CTs nanoparticles and LED light spectra, along with the optimization of plant growth regulators, provides a promising method for enhancing the production of valuable secondary metabolites, such as thymoquinone, in black cumin callus cultures. Future research in this area has the potential to unlock new pathways for the industrial-scale production of bioactive compounds from medicinal plants, contributing to the development of sustainable, plant-based pharmaceuticals and bioactive products.

Materials and methods

Synthesis of Fe-CTs NPs

Using the in-situ approach, Fe^{2+}/Fe^{3+} ions were initially collected during the co-precipitation procedure in order to manufacture magnetized chitosan. 100 mL of 1% (w/w) acetic acid solution was used to dissolve 1 g of chitosan powder (Beijing Be-Better Technology Co., Ltd., Beijing, China) and the mixture was then heated to 70 °C. Following an hour of stirring, the chitosan solution was supplemented with 2 g of $FeCl_2{\cdot}4H_2O$ and 5.4 g of $FeCl_3{\cdot}6H_2O$ iron salts (nFe^{3+}/nFe^{2+} = 2) that had been dissolved in 20 mL of distilled water.

For thirty minutes, the resultant solution was purified using inert nitrogen gas. Next, dropwise addition of 3 M ammonia solution was made until the pH of the purified solution reached 11. The dark chitosan solution loaded with Fe^{2+}/Fe^{3+} demonstrated the formation of Fe_3O4 nanoparticles. It was then agitated for a full hour at 70 °C. The obtained solution underwent purification to get rid of excess material that hadn't reacted from the reaction medium. The pH of the solution was 7 following multiple washes with more distilled water. Using an ultrasonic device set to 50 Hz for 30 min, an equal amount of magnetized chitosan was mixed with 100 mL of distilled water to create a homogenous solution from the preserved sample. Next, a magnet was used to separate the Fe^{2+}/Fe^{3+} loaded chitosan, and the material was dried using a freeze-drying procedure [33].

Plant materials and cultivation

Nigella sativa seeds were collected by the Seed and Seedling Research Institute and then sterilized with running water, the fungicide mancozeb (100 mg L^{-1}), 70% ethanol, and 2.5% sodium hypochlorite (NaClO) for 6 h, 2 h, 30 s, and 6–7 min, respectively then the seeds were washed again 3 times with deionized distilled water to reduce the harmful effects of bleach and ethanol. Disinfected sample in MS (Murashige and Skoog) base culture medium with five replicates under in vitro conditions when treated with 2,4-dichlorophenoxyacetic acid 2,4-D (0, 1, 2 and 4 mg L^{-1}) and 6-benzylaminopurine BAP (0, 0.5, 1 and 2 mg L^{-1}) in with a photoperiod of 16 h of light and 8 h of darkness, with a photosynthetic intensity of 2000 lx at 20–24 ∘C.

After finding the best PGR combination for propagation, several subcultures were established to obtain maximum callus. The plants were cultivated in MS medium containing four concentrations of FeO_3-CTs nanoparticles under four different light treatments with a light intensity of 2000 lx.

This project was conducted in the tissue culture laboratory of the Department of Horticultural Sciences, Faculty of Agriculture, University of Mohaghegh Ardabili, Ardabil, Iran.

Stimulation of callus with LED light quality

Under aseptic conditions, the weight of healthy growing callus on solidified MS medium (Murashige Skoog) was measured as 1 g utilizing a precision scale and subsequently relocated to MS medium enriched with the best PGR treatment (2 mg L^{-1} 2,4-D and 1 mg L^{-1} BAP) with 30 g L^{-1} sucrose and solidified with 7 g L^{-1} agar. For LED light quality treatment, 3 light qualities and also in dark conditions Dark (D), White (W, 450–640 nm), Blue (B, 450 nm) and Red (R, 640 nm) with light intensity of 2000 lx were used, and for nanoparticle FeO_3-CTs treatment, four concentrations (0, 50, 100, 200 mg L^{-1}) were used as a factorial experiment in the form of a completely randomized basic experiment with five replicates.

First, the initial weight of the culture medium without callus was measured as a control, then the wet weight and the size of the callus were measured weekly, and at the end of the experiment, four replicates were taken from each treatment to determine the dry weight and type of callus tissue. On the other hand, to measure and analyze other factors, such as the amount of thymoquinone, metabolites, growth parameters, etc. callus were harvested and quickly pulverized in liquid nitrogen and then stored in a refrigerator at -72 ° C.

Determination of callus growth parameters

After the treatment period, the callus harvested was cleaned from all treatments of MS medium enriched nutrient. The initial step involved determined the fresh weight (FW) using sterile paper on the balance was done. Fresh weights were determined to calculate the growth index of the callus. After that, the calluses were placed in an oven at a temperature of 40 °C for 2 days and the dry weight was obtained. The following formula was used:

$$Growthindex = \left(harvestedFW\,(g) - inoculatedFW\,(g)\right) / inoculatedFW\,(g)$$

Preparation of dry matter for assay

After drying the calluses, we ground them and to prepare stock, we mixed 100 mg in 5 ml of methanol (20/80) and put it on a shaker for 24 h. Then, the solvent was evaporated using filter paper and rotary evaporation, and finally stored in the refrigerator [79].

Total phenolic and flavonoid content

The TPC was evaluated based on the ways described by of Meda et al. [62] (the equivalent of gallic acid per gram dry weight of the plant) [62].

The TFC was assessed using the methods explained by Mita et al. [66]. For this purpose, 2 ml of Methanol (80%) with 150 µl of Sodium acetate solution (1 mol), 150 µl of $Alcl_3$ solution and 2.8 ml of distilled water were used. The absorbance of was read in the wavelength range of 415 nm. For TFC, Quercetin was applied as standard. TFC was stated as mg quercetin equivalent per gram DM of the plant [66].

Total antioxidant capacity (TAC)(DPPH)

The TAC calculated according ways of Miliauskas et al. [65]. different concentrations (the final weight ratio of the solution in DPPH was nearly 3;1, 1.5;1, 0.75:1) of the extract were mixed with 2 mL of a 0.023% methanolic solution. The control solution contained 2 mL DPPH and 2 mL methanol. The solutions were stored in the dark at room temperature for 30 min. The absorbance of the samples was detected at 517 nm compared to the methanol control [65]. Antioxidant activity was calculated based on inhibition (%) using the following formula:

$$I\% = \left(Acontrol - Asample\right) / Acontrol \times 100$$

Total carbohydrates (TCc)

In this study, the phenol-sulfuric acid method was used to measure total carbohydrates (TCc) in the samples. A standard curve was established using glucose at concentrations ranging from 0 to 10 mg per 100 mL, The amount of TC was then calculated in mg g-1 of the dry weight of the samples. The protocol used was described by Irigoyen [31, 44].

Extraction of Gallic acid and Quercetin from callus

The procedure was performed according to those explained by [48] To analyze quercetin and gallic acid in the callus induced by N. sativa, the dried plants were ground to a powder with a pestle. 10 ml methanol was applied for analysis.

The methanol solution was sonicated for three times. Then it was centrifuged at 2000 rpm for 10 min. A rotary was used to evaporate the supernatants at 45 °C. Then, 800 µl of methanol was added. Finally, the extracts were filtered using 0.45 µm filter.

Measurement of quercetin and gallic acid using a spectrophotometric method

The prepared solutions of quercetin and gallic acid were at precise concentrations of 0.25, 0.5, 1, 2 and 4 mg per 100 ml. The absorbance spectra of the two substances were determined using a Thermo Fisher spectrophotometer (ND One, USA) and the maximum absorbance values were recorded. Using the concentration of the standard solutions of quercetin and gallic acid and the absorbance values as the y-coordinate, a linear regression analysis was performed to generate calibration curves for both substances. The results showed that the absorption maximum of quercetin occurred at a wavelength of

405 nm, for gallic acid it was at a wavelength of 310 nm [92].

Determination of thymoquinone (TQ) by GC-MS

Preparation of samples and gas chromatography

Monoterpenoids where analyzed on triple-quad GC-MS Scion 8900. In brief, fresh sample of callus was mix with 700 ml of acetone, homogenized and extracted in ultrasound bath in temp. 20 °C for 30 min. We did not decide for drying, to avoid the loses in volatiles during process. Next, sample was centrifuged (5 min, 14,000 g) and organic phase was collected. Extraction was repeated two times. Collected organic phases where dried over anhydrous Na_2SO_4, and submitted into the gas chromatography. One mL of sample was injected on GC-MS in MRM mode. Temperature ramp where as follow: 60 °C in 1 min, next 8 °C/min to 180 °C and finally 18 °C/min to 240 with hold time 4 min. Injector was set on 225 °C with split ratio 5. Signals where analyzed in MRM mode (precursor 164, product 149, collision energy 5 eV, with standard, 2 quadrupole 1 and quadrupole 3 resolution. Polarity was set as positive. Separation was performed on SH-5 column (Shimadzu, Kyoto, Japan) 30 m x 0,25 mm x 0,25 mm film thickness). Quantification was based on calibration curves.

Statistical analyses

The factorial test data were recorded using a completely randomized design in Excel and subsequently analyzed with SAS 9.1 software. Statistical analysis was conducted at probability levels of 1% and 5% to determine the significance of the results.

Acknowledgements

We appreciate University of Mohaghegh Ardabili, Ardabil, Iran for providing preliminary materials. We also thank Wrocław University of Environmental and Life Sciences, Poland for supporting this study. We appreciate University of Mohaghegh Ardabili, Ardabil, Iran for providing preliminary materials. We also thank Wrocław University of Environmental and Life Sciences, Poland for supporting this study.

Author contributions

M.T, M.B, A.S, M.M, A.Sz contributed to the design of the study, validation, data interpretation, and writing-review and editing. A.S., performed the writing-original draft preparation, analyzed the data, and wrote the initial draft of the article. interpretation as well as editing of the final version of the manuscript. All authors have read and agreed to the published version of the manuscript.

Funding

Not applicable.

Data availability

No datasets were generated or analysed during the current study.

Declarations

Ethics approval and consent to participate

All methods performed in this study including the plant tissue culture were in compliance with the relevant institutional, national, and international guidelines and legislation.

Consent for publication

Not applicable.

Statement of compliance

The authors confirm that all the experimental research and in vitro studies on *Nigella sativa* callus, including plants sample, complied with relevant institutional, national, and international guidelines and legislation. Also, obtained licenses of tissue culture plants of Black cumin.

Statement on experimental research and field studies on plants

The Tissue culture of Nigella sativa sampled comply with relevant institutional, national, and international guidelines and domestic legislation of Iran.

Statement specifying permissions

In this study, we obtained permission to in vitro plants tissue culture if issued by the Agricultural and Natural Resources and science Ministry of Iran.

Competing interests

The authors declare no competing interests.

Author details

[1]Department of Horticultural Sciences, Faculty of Agriculture and Natural Resources, University of Mohaghegh Ardabili, Ardabil 56199-11367, Iran
[2]Department of Plant Production and Genetics, Faculty of Agriculture, University of Kurdistan, P. O. Box 416, Sanandaj, Iran
[3]Department of Food Chemistry and Biocatalysis, Wrocław University of Environmental and Life Sciences, Wrocław, Poland

Received: 21 September 2024 / Accepted: 18 March 2025
Published online: 25 April 2025

References

1. Adil M, Ren X, Kang DI, Thi LT, Jeong BR. Effect of explant type and plant growth regulators on callus induction, growth and secondary metabolites production in Cnidium officinale Makino. Mol Biol Rep. 2018;45:1919–27.
2. Aftab A, Yousaf Z, Shamsheer B, Riaz N, Rashid M, Younas A, Javaid A. Thymoquinone: biosynthesis, biological activities and therapeutic potential from natural and synthetic sources. Int J Agric Biology. 2021;25(5):1024–34.
3. Ahmad A, Mishra RK, Vyawahare A, Kumar A, Rehman MU, Qamar W, Khan AQ, Khan R. Thymoquinone (2-Isopropyl-5-methyl-1, 4-benzoquinone) as a chemopreventive/anticancer agent: chemistry and biological effects. Saudi Pharm J. 2019;27(8):1113–26.
4. Ahmadianfar S, Mehrabi N, Mohammadi S, Sobhanizadeh A, Moradabadi A, Noroozi-Aghideh A. Effects of Horsetail, Alfalfa, Ortie, Chêne and Aleppo oak as potential hemostatic agents on laboratory coagulation tests. Nat Prod Sci. 2023;29(1):42–9.
5. Ahmadianfar S, Sabiza S, Sobhanizadeh A, Noroozi-Aghideh A. Anti-Hemorrhagic effect of Horsetail, Ortie, Alfalfa, Chêne, and Aleppo Oakin an experimental model of Rats-a potential theoretic approach for traumatic bleeding. J Cell Mol Anesth. 2021;6(2):111–8.
6. Ahmadpoor F, Zare N, Asghari R, Sheikhzadeh-Mosadeg P. The effect of plant growth regulators on the antioxidant enzyme activity and secondary metabolite production in the cell suspension cultures of melia Azedarach L. J Hortic Sci Biotechnol. 2023;98(5):662–77.
7. Ahmed ZM, Attia MS, Mahmoud AM, Shoreibah EA. Evaluation of topical application of Nigella sativa (black seeds) on delayed dental implant. Al-Azhar Dent J Girls. 2020;7(2–B):255–61.
8. Al-Hussaini Z, Yousif S, Al-Ajeely S. Effect of different medium on callus induction and regeneration in potato cultivars. Int J Curr Microbiol Appl Sci. 2015;4(5):856–65.
9. Alam P, Shakeel F, Taleuzzaman M, Foudah AI, Alqarni MH, Aljarba TM, Alshehri S, Ghoneim MM. Box-Behnken design (BBD) application for optimization of chromatographic conditions in RP-HPLC method development for the Estimation of thymoquinone in Nigella sativa seed powder. Processes. 2022;10(6):1082.
10. Ali AMA, El-Nour MEM, Yagi SM. Total phenolic and flavonoid contents and antioxidant activity of ginger (Zingiber officinale Rosc.) rhizome, callus and callus treated with some elicitors. J Genetic Eng Biotechnol. 2018;16(2):677–82.

11. Anaeigoudari A, Safari H, Khazdair MR. Effects of Nigella sativa, camellia sinensis, and allium sativum as food additives on metabolic disorders, a literature review. Front Pharmacol. 2021;12:762182.
12. Appu M, Lian Z, Zhao D, Huang J. Biosynthesis of chitosan-coated iron oxide (Fe 3 O 4) hybrid nanocomposites from leaf extracts of brassica Oleracea L. and study on their antibacterial potentials. 3 Biotech. 2021;11:1–14.
13. Azizi N, Amini MR, Djafarian K, Shab-Bidar S. The effects of Nigella sativa supplementation on liver enzymes levels: A systematic review and meta-analysis of randomized controlled trials. Clin Nutr Res. 2021;10(1):72.
14. Badary OA, Hamza MS, Tikamdas R. (2021). Thymoquinone: A promising natural compound with potential benefits for COVID-19 prevention and cure. *Drug design, development and therapy*, 1819–1833.
15. Benková E, Michniewicz M, Sauer M, Teichmann T, Seifertová D, Jürgens G, Friml J. Local, efflux-dependent auxin gradients as a common module for plant organ formation. Cell. 2003;115(5):591–602.
16. Binte Mostafiz S, Wagiran A. Efficient callus induction and regeneration in selected indica rice. Agronomy. 2018;8(5):77.
17. Bong FJ, Chear NJY, Ramanathan S, Mohana-Kumaran N, Subramaniam S, Chew BL. The development of callus and cell suspension cultures of Sabah snake grass (Clinacanthus nutans) for the production of flavonoids and phenolics. Biocatal Agric Biotechnol. 2021;33:101977.
18. Cavallaro V, Pellegrino A, Muleo R, Forgione I. Light and plant growth regulators on in vitro proliferation. Plants. 2022;11(7):844.
19. Dalli M, Azizi S-e, Benouda H, Azghar A, Tahri M, Bouammali B, Maleb A, Gseyra N. Molecular composition and antibacterial effect of five essential oils extracted from Nigella sativa L. seeds against multidrug-resistant bacteria: a comparative study. Evid Based Complement Alternat Med. 2021.
20. Danaei GH, Memar B, Ataee R, Karami M. Protective effect of thymoquinone, the main component of Nigella sativa, against Diazinon cardio-toxicity in rats. Drug Chem Toxicol. 2019;42(6):585–91.
21. Elyasi R, Majdi M, Krause ST, Kücükay N, Azizi A, Degenhardt J. Identification and functional characterization of a γ-terpinene synthase in Nigella sativa L (black cumin). Phytochemistry. 2022;202:113290.
22. Esharkawy ER, Almalki F, Hadda TB. In vitro potential antiviral SARS-CoV-19-activity of natural product thymohydroquinone and dithymoquinone from Nigella sativa. Bioorg Chem. 2022;120:105587.
23. Etheve S, Prudence K, Schweikert L, Szepes A. Capsules containing thymoquinone. In: Google Patents; 2015.
24. Fahimirad S, Ajalloueian F, Ghorbanpour M. Synthesis and therapeutic potential of silver nanomaterials derived from plant extracts. Ecotoxicol Environ Saf. 2019;168:260–78.
25. Fazal H, Abbasi BH, Ahmad N, Ali M, Shujait Ali S, Khan A, Wei D-Q. Sustainable production of biomass and industrially important secondary metabolites in cell cultures of selfheal (Prunella vulgaris L.) elicited by silver and gold nanoparticles. Artif Cells Nanomed Biotechnol. 2019;47(1):2553–61.
26. Fazeli-Nasab B, Shahraki-Mojahed L, Piri R, Sobhanizadeh A. Trichoderma: improving growth and tolerance to biotic and abiotic stresses in plants. Trends of applied microbiology for sustainable economy. Elsevier; 2022. pp. 525–64.
27. Fazeli-Nasab B, Solouki M, Sobhanizadeh A. Green synthesis of silver nanoparticles using an ephedra sinica herb extract with antibacterial properties. J Med Bacteriol. 2021:30-47.
28. Fehér A. Callus, dedifferentiation, totipotency, somatic embryogenesis: what these terms mean in the era of molecular plant biology? Front Plant Sci. 2019;10:536.
29. FILOVÁ A. Production of secondary metabolities in plant tissue cultures. Res J Agricultural Sci 2014:46(1).
30. Foster S, Duke JA. A field guide to medicinal plants and herbs of Eastern and central North America. Houghton Mifflin Harcourt; 2000(2).
31. Gharibi S, Matkowski A, Sarfaraz D, Mirhendi H, Fakhim H, Szumny A, Rahimmalek M. Identification of polyphenolic compounds responsible for antioxidant, anti-Candida activities and nutritional properties in different pistachio (Pistacia Vera L.) hull cultivars. Molecules. 2023;28(12):4772.
32. Gharibi S, Tabatabaei BES, Saeidi G, Talebi M, Matkowski A. The effect of drought stress on polyphenolic compounds and expression of Flavonoid biosynthesis related genes in Achillea pachycephala Rech. F. Phytochemistry. 2019;162:90–8.
33. Giglou MT, Giglou RH, Esmaeilpour B, Azarmi R, Padash A, Falakian M, Śliwka J, Gohari G, Lajayer HM. A new method in mitigation of drought stress by chitosan-coated iron oxide nanoparticles and growth stimulant in peppermint. Ind Crops Prod. 2022;187:115286.
34. Giglou RH, Giglou MT, Esmaeilpour B, Padash A, Ghahremanzadeh S, Sobhanizade A, Hatami M. Exogenous melatonin differentially affects biomass, total carbohydrates, and essential oil production in peppermint upon simultaneous exposure to chitosan-coated Fe3O4 NPs. South Afr J Bot. 2023;163:135–44.
35. Giglou RH, Giglou MT, Estaji A, Bovand F, Ghorbanpour M. Light-emitting diode irradiation and Glycine differentially affect photosynthetic performance of black Henbane (Hyoscyamus Niger L). South Afr J Bot. 2023;155:230–40.
36. Golpour-Hamedani S, Hadi A, SafariMalekabadi D, Najafgholizadeh A, Askari G, Pourmasoumi M. The effect of Nigella supplementation on blood pressure: A systematic review and dose-response meta-analysis. Crit Rev Food Sci Nutr. 2022:1-14.
37. Gyawali D, Vohra R, Orme-Johnson D, Ramaratnam S, Schneider RH. A systematic review and meta-analysis of ayurvedic herbal preparations for hypercholesterolemia. Medicina. 2021;57(6):546.
38. Haftador HM, Ramhormozi P, Yousefpour M, Sobhanizadeh A, Ghahari L. Healing effects of Iranian Dwarf elder on Full-thickness epidermal thermal injury in Wistar rats. Annals Military Health Sci Res 2021:19(4).
39. Halder M, Sarkar S, Jha S. Elicitation: A biotechnological tool for enhanced production of secondary metabolites in hairy root cultures. Eng Life Sci. 2019;19(12):880–95.
40. Hartati H, Subaer S, Hasri H, Wibawa T, Hasriana H. Microstructure and antibacterial properties of chitosan-Fe3O4-AgNP nanocomposite. Nanomaterials. 2022;12(20):3652.
41. Hassan ST, Šudomová M. Comment on: effects of Nigella sativa on type-2 diabetes mellitus: A systematic review. Int J Environ Res Public Health. 2020;17(5):1630.
42. Huang J, Cheng Z-H, Xie H-H, Gong J-Y, Lou J, Ge Q, Wang Y-J, Wu Y-F, Liu S-W, Sun P-L. Effect of quaternization degree on physiochemical and biological activities of Chitosan from squid pens. Int J Biol Macromol. 2014;70:545–50.
43. Huang X, Yao J, Zhao Y, Xie D, Jiang X, Xu Z. Efficient Rutin and Quercetin biosynthesis through flavonoids-related gene expression in fagopyrum Tataricum Gaertn. Hairy root cultures with UV-B irradiation. Front Plant Sci. 2016;7:63.
44. Irigoyen J, Einerich D, Sánchez-Díaz M. Water stress induced changes in concentrations of proline and total soluble sugars in nodulated alfalfa (Medicago sativa) plants. Physiol Plant. 1992;84(1):55–60.
45. Irshad M, Liu W, Wang L, Shah SBH, Sohail MN, Uba MM. Li-local: green communication modulations for indoor localization. Proceedings of the 2nd International Conference on Future Networks and Distributed Systems 2018.
46. Isah B, Mustapha Y, Sani L. Effect of types and concentrations of auxins on callus induction and primary somatic embryogenesis in low cyanide cassava cultivars (Manihot esculentum Cranz). Bayero J Pure Appl Sci. 2018;11(1):497–501.
47. Jafari H, Atlasi Z, Mahdavinia GR, Hadifar S, Sabzi M. Magnetic κ-carrageenan/chitosan/montmorillonite nanocomposite hydrogels with controlled Sunitinib release. Mater Sci Engineering: C. 2021;124:112042.
48. Jakabová S, Vincze L, Farkas Á, Kilár F, Boros B, Felinger A. Determination of tropane alkaloids Atropine and scopolamine by liquid chromatography–mass spectrometry in plant organs of Datura species. J Chromatogr A. 2012;1232:295–301.
49. Jan R, Khan MA, Asaf S, Lee I-J, Kim K-M. Modulation of sugar and nitrogen in callus induction media alter PAL pathway, SA and biomass accumulation in rice callus. Plant Cell Tissue Organ Cult (PCTOC). 2020;143:517–30.
50. Kabir Y, Shirakawa H, Komai M. Nutritional composition of the Indigenous cultivar of black Cumin seeds from Bangladesh. Prog Nutr. 2019;21:428–34.
51. Khader M, Eckl PM. Thymoquinone: an emerging natural drug with a wide range of medical applications. Iran J Basic Med Sci. 2014;17(12):950.
52. Kolewe ME, Gaurav V, Roberts SC. Pharmaceutically active natural product synthesis and supply via plant cell culture technology. Mol Pharm. 2008;5(2):243–56.
53. Kumandaş A, Karslı B, Kürüm A, Çınar M, Elma E. Comparison of the effects of zinc-silver cream and Nigella sativa oil on wound healing and oxidative stress in the wound model in rats 2020.
54. Kumari A, Naidoo D, Baskaran P, Doležal K, Nisler J, Van Staden J. Phenolic and flavonoid production and antimicrobial activity of gymnosporia buxifolia (L.) Szyszyl cell cultures. Plant Growth Regul. 2018;86:333–8.
55. Lee D-H, Sim G-S, Kim J-H, Lee G-S, Pyo H-B, Lee B-C. Preparation and characterization of quercetin-loaded polymethyl methacrylate microcapsules using a polyol-in-oil-in-polyol emulsion solvent evaporation method. J Pharm Pharmacol. 2007;59(12):1611–20.

56. Lee S-W, Seo JM, Lee M-K, Chun J-H, Antonisamy P, Arasu MV, Suzuki T, Al-Dhabi NA, Kim S-J. Influence of different LED lamps on the production of phenolic compounds in common and Tartary buckwheat sprouts. Ind Crops Prod. 2014;54:320–6.
57. Lian X, Wang X, Ling Y, Lochner E, Tan L, Zhou Y, Ma B, Hanson K, Gao H. Light emitting diodes based on inorganic composite halide perovskites. Adv Funct Mater. 2019;29(5):1807345.
58. Limpanavech P, Chaiyasuta S, Vongpromek R, Pichyangkura R, Khunwasi C, Chadchawan S, Lotrakul P, Bunjongrat R, Chaidee A, Bangyeekhun T. Chitosan effects on floral production, gene expression, and anatomical changes in the dendrobium Orchid. Sci Hort. 2008;116(1):65–72.
59. Malerba M, Cerana R. Recent applications of chitin-and chitosan-based polymers in plants. Polymers. 2019;11(5):839.
60. Mamdouh D, Smetanska I. Optimization of callus and cell suspension cultures of lycium schweinfurthii for improved production of phenolics, flavonoids, and antioxidant activity. Horticulturae. 2022;8(5):394.
61. Martysiak-Żurowska D, Wenta W. A comparison of ABTS and DPPH methods for assessing the total antioxidant capacity of human milk. Acta Scientiarum Polonorum Technologia Aliment. 2012;11(1):83–9.
62. Meda A, Lamien CE, Romito M, Millogo J, Nacoulma OG. Determination of the total phenolic, flavonoid and proline contents in Burkina Fasan honey, as well as their radical scavenging activity. Food Chem. 2005;91(3):571–7.
63. Mendoza D, Arias JP, Cuaspud O, Arias M. Phytochemical screening of callus and cell suspensions cultures of Thevetia peruviana. Braz Arch Biol Technol. 2020:63.
64. Mierziak J, Kostyn K, Kulma A. Flavonoids as important molecules of plant interactions with the environment. Molecules. 2014;19(10):16240–65.
65. Miliauskas G, Venskutonis P, Van Beek T. Screening of radical scavenging activity of some medicinal and aromatic plant extracts. Food Chem. 2004;85(2):231–7.
66. Mita S, Murano N, Akaike M, Nakamura K. Mutants of Arabidopsis Thaliana with pleiotropic effects on the expression of the gene for β-amylase and on the accumulation of anthocyanin that are inducible by sugars. Plant J. 1997;11(4):841–51.
67. Mohammed AE. Green synthesis, antimicrobial and cytotoxic effects of silver nanoparticles mediated by Eucalyptus camaldulensis leaf extract. Asian Pac J Trop Biomed. 2015;5(5):382–6.
68. Mok DW, Mok MC. Cytokinin metabolism and action. Annu Rev Plant Biol. 2001;52(1):89–118.
69. Monica RC, Cremonini R. Nanoparticles and higher plants. Caryologia. 2009;62(2):161–5.
70. Montazeri RS, Fatahi S, Sohouli MH, Abu-Zaid A, Santos HO, Găman MA, Shidfar F. The effect of Nigella sativa on biomarkers of inflammation and oxidative stress: A systematic review and meta-analysis of randomized controlled trials. J Food Biochem. 2021;45(4):e13625.
71. Morales LO, Tegelberg R, Brosche M, Keinänen M, Lindfors A, Aphalo PJ. Effects of solar UV-A and UV-B radiation on gene expression and phenolic accumulation in betula pendula leaves. Tree Physiol. 2010;30(7):923–34.
72. Murthy HN, Lee E-J, Paek K-Y. Production of secondary metabolites from cell and organ cultures: strategies and approaches for biomass improvement and metabolite accumulation. Plant Cell Tissue Organ Cult (PCTOC). 2014;118:1–16.
73. Nanya K, Ishigami Y, Hikosaka S, Goto E. (2012). Effects of blue and red light on stem elongation and flowering of tomato seedlings. VII International Symposium on Light in Horticultural Systems 2012:956.
74. Narayani M, Srivastava S. Elicitation: a stimulation of stress in in vitro plant cell/tissue cultures for enhancement of secondary metabolite production. Phytochem Rev. 2017;16:1227–52.
75. Nguyen MD, Tran H-V, Xu S, Lee TR. Fe3O4 nanoparticles: structures, synthesis, magnetic properties, surface functionalization, and emerging applications. Appl Sci. 2021;11(23):11301.
76. Ochoa-Villarreal M, Howat S, Hong S, Jang MO, Jin Y-W, Lee E-K, Loake GJ. Plant cell culture strategies for the production of natural products. BMB Rep. 2016;49(3):149.
77. Ozyigit II, Gozukirmizi N, Semiz BD. Genotype dependent callus induction and shoot regeneration in sunflower (Helianthus annuus L.). Afr J Biotechnol. 2007;6(13).
78. Peng LX, Zou L, Su YM, Fan Y, Zhao G. Effects of light on growth, levels of anthocyanin, concentration of metabolites in fagopyrum Tataricum sprout cultures. Int J Food Sci Technol. 2015;50(6):1382–9.
79. Pourmorad F, Hosseinimehr S, Shahabimajd N. Antioxidant activity, phenol and flavonoid contents of some selected Iranian medicinal plants. Afr J Biotechnol, 2006:5(11).
80. Rafeie M, Shabani L, Sabzalian MR, Gharibi S. Pretreatment with leds regulates antioxidant capacity and polyphenolic profile in two genotypes of Basil under salinity stress. Protoplasma. 2022;259(6):1567–83.
81. Rahayu S, Roostika I, Bermawie N. The effect of types and concentrations of auxins on callus induction of centella Asiatica. Nusantara Bioscience. 2016;8(2):283–7.
82. Rajila M, Arunprasath A. IN-VITRO REGENERATION, FLOWERING & GC-MS ANALYSIS IN CALLUS OF LINDERNIA MADAYIPARENSE-AN ENDEMIC PLANT TO MADAYIPARA, KERALA, INDIA. Int J Conserv Sci. 2020;11(3):783–90.
83. Ramakrishna A, Ravishankar GA. Influence of abiotic stress signals on secondary metabolites in plants. Plant Signal Behav. 2011;6(11):1720.
84. Robles-Martínez M, Barba-de La Rosa AP, Guéraud F, Negre-Salvayre A, Rossignol M, Santos-Díaz MdS. Establishment of callus and cell suspensions of wild and domesticated opuntia species: study on their potential as a source of metabolite production. Plant Cell Tissue Organ Cult (PCTOC). 2016;124:181–9.
85. Rodríguez-Calzada T, Qian M, Strid Å, Neugart S, Schreiner M, Torres-Pacheco I, Guevara-González RG. Effect of UV-B radiation on morphology, phenolic compound production, gene expression, and subsequent drought stress responses in Chili pepper (Capsicum annuum L). Plant Physiol Biochem. 2019;134:94–102.
86. Ruttkay-Nedecky B, Krystofova O, Nejdl L, Adam V. Nanoparticles based on essential metals and their phytotoxicity. J Nanobiotechnol. 2017;15(1):1–19.
87. Ryan KG, Swinny EE, Markham KR, Winefield C. Flavonoid gene expression and UV photoprotection in Transgenic and mutant Petunia leaves. Phytochemistry. 2002;59(1):23–32.
88. Saidin KS, Jais MR, Ismail EN, Ishak R. The effect of Nigella sativa and eucheuma Cottonii in collagen-induced arthritis mice 2020.
89. Saif S, Hanif M, Rehman R, Riaz M. Garlic. Medicinal plants of South Asia. In: Amsterdam: Elsevier; 2020.
90. Sajfrtova M, Sovova H, Karban J. Enrichment of Nigella Damascena extract with volatile compounds using supercritical fluid extraction. J Supercrit Fluids. 2014;94:160–4.
91. Saraswat AL, Maher TJ. Development and optimization of stealth liposomal system for enhanced in vitro cytotoxic effect of Quercetin. J Drug Deliv Sci Technol. 2020;55:101477.
92. Sarfaraz D, Rahimmalek M, Sabzalian MR, Gharibi S, Matkowski A, Szumny A. Essential oil composition and antioxidant activity of oregano and marjoram as affected by different Light-Emitting diodes. Molecules. 2023;28(9):3714.
93. Shah P, Modi H. Comparative study of DPPH, ABTS and FRAP assays for determination of antioxidant activity. Int J Res Appl Sci Eng Technol. 2015;3(6):636–41.
94. Shahbazi E, Safipor B, Golkar P. Responses of Nigella Damascena L. and Nigella sativa L. to drought stress: yield, fatty acid composition and antioxidant activity. J Agricultural Sci Technol. 2022;24(3):693–705.
95. Shanmugam MK, Arfuso F, Kumar AP, Wang L, Goh BC, Ahn KS, Bishayee A, Sethi G. Modulation of diverse oncogenic transcription factors by thymoquinone, an essential oil compound isolated from the seeds of Nigella sativa Linn. Pharmacol Res. 2018;129:357–64.
96. Shirsat R, Kengar A, Rai A. In-vitro callogenesis and screening of antimicrobial activity of callus and seed of caesalpinia Bonducella F.: A threatened medicinal plant of Western Ghats. J Pharm Res Int. 2021;33(31A):76–89.
97. Silveira D, Boylan F. Medicinal plants: advances in phytochemistry and ethnobotany. Volume 12. MDPI; 2023. p. 1682.
98. Sobhanizadeh A. Optimization of callus induction investigating the effect of biotic and abiotic elicitors on amount of phenols compound of medicinal plant Nigella sativa in vitro University of Zabol] 2016.
99. Sobhanizadeh A, Solouki M, Bahman Fazeli-Nasab B. Optimization of callus induction and effects of biological and non-biological elicitors on content of phenol/flavonoid compounds in Nigella sativa under in-vitro conditions. Cell Tissue J. 2017;8(2):165–84.
100. Soleymani S, Zargaran A, Farzaei MH, Iranpanah A, Heydarpour F, Najafi F, Rahimi R. The effect of a hydrogel made by Nigella sativa L. on acne vulgaris: A randomized double-blind clinical trial. Phytother Res. 2020;34(11):3052–62.
101. Sun M, Gu X, Fu H, Zhang L, Chen R, Cui L, Zheng L, Zhang D, Tian J. Change of secondary metabolites in leaves of Ginkgo Biloba L. in response to UV-B induction. Innovative Food Sci Emerg Technol. 2010;11(4):672–6.
102. Tiji S, Bouhrim M, Addi M, Drouet S, Lorenzo JM, Hano C, Bnouham M, Mimouni M. Linking the phytochemicals and the α-glucosidase and

α-amylase enzyme inhibitory effects of Nigella sativa seed extracts. Foods. 2021;10(8):1818.
103. Tiwari A, Surendra G, Meka S, Varghese B, Vishwakarma G, Adela R. The effect of Nigella sativa on non-alcoholic fatty liver disease: A systematic review and meta-analysis. Hum Nutr Metabolism. 2022;28:200146.
104. Uysal H. In vitro propagation of black Cumin (Nıgella Satıva L.) plants. Genetika. 2021;53(1):295–303.
105. Uysal H, Sevindik E. Development of breeding lines by zigotic ovule culture in Nigella sativa L. Genetika. 2021;53(2):583–91.
106. Verma SK, Gantait S, Mukherjee E, Gurel E. Enhanced somatic embryogenesis, plant regeneration and total phenolic content Estimation in lycium barbarum L.: a highly nutritive and medicinal plant. J Crop Sci Biotechnol. 2022;25(5):547–55.
107. Verpoorte R, Alfermann AW. Metabolic engineering of plant secondary metabolism. Springer Science & Business Media; 2000.
108. Verpoorte R, Contin A, Memelink J. Biotechnology for the production of plant secondary metabolites. Phytochem Rev. 2002;1:13–25.
109. Wang P, Lombi E, Zhao F-J, Kopittke PM. Nanotechnology: a new opportunity in plant sciences. Trends Plant Sci. 2016;21(8):699–712.
110. Yasuda T, Fujii Y, Yamaguchi T. Embryogenic callus induction from coffea Arabica leaf explants by benzyladenine. Plant Cell Physiol. 1985;26(3):595–7.
111. Yetkin NA, Büyükoğlan H, Sönmez MF, Tutar N, Gülmez I, Yilmaz I. The protective effects of thymoquinone on lung damage caused by cigarette smoke. Biotech Histochem. 2020;95(4):268–75.
112. Yimer EM, Tuem KB, Karim A, Ur-Rehman N, Anwar F. Nigella sativa L.(black cumin): a promising natural remedy for wide range of illnesses. Evid Based Complement Alternat Med. 2019.
113. Yuan Y, Chesnutt BM, Haggard WO, Bumgardner JD. Deacetylation of Chitosan: material characterization and in vitro evaluation via albumin adsorption and pre-osteoblastic cell cultures. Materials. 2011;4(8):1399–416.
114. Yue W, Ming Q-l, Lin B, Rahman K, Zheng C-J, Han T, Qin L-p. Medicinal plant cell suspension cultures: pharmaceutical applications and high-yielding strategies for the desired secondary metabolites. Crit Rev Biotechnol. 2016;36(2):215–32.
115. Zaman MAK, Azzeme AM, Ramle IK, Normanshah N, Ramli SN, Shaharuddin NA, Ahmad S, Abdullah SN. A. Induction, multiplication, and evaluation of antioxidant activity of polyalthia bullata callus, a Woody medicinal plant. Plants, 2020:9(12).
116. Zhang R, Wu T, Zheng P, Liu M, Xu G, Xi M, Yu J. RETRACTED: thymoquinone sensitizes human hepatocarcinoma cells to TRAIL-induced apoptosis via oxidative DNA damage. In: Elsevier; 2021.
117. Adinew GM, Taka E, Mochona B, Badisa RB, Mazzio EA, Elhag R, Soliman KF. Therapeutic potential of thymoquinone in triple-negative breast cancer prevention and progression through the modulation of the tumor microenvironment. Nutrients. 2021;14(1):79.
118. Alu'datt MH, Rababah T, Al-u'datt DAG, Gammoh S, Alkandari S, Allafi A, Al-Rashdan HK. Designing novel industrial and functional foods using the bioactive compounds from Nigella sativa L.(black cumin): Biochemical and biological prospects toward health implications. J Food Sci. 2024;89(4):1865–93.
119. Heydarnajad Giglou R, Torabi Giglou M, Estaji A, Moradian H. LED lights and Glycine promote biomass, leaf color changes, and secondary metabolites accumulation in hyoscyamus Niger L. Int J Hortic Sci Technol. 2025;12(2):569–82.
120. Jan R, Aaqil Khan M, Asaf S, Lubna, Park JR, Lee IJ, Kim KM. Flavonone 3-hydroxylase relieves bacterial leaf blight stress in rice via overaccumulation of antioxidant flavonoids and induction of defense genes and hormones. Int J Mol Sci. 2021;22(11):6152.
121. Pashkovskiy PP, Soshinkova TN, Korolkova DV, Kartashov AV, Zlobin IE, Lyubimov VY, Kuznetsov VV. The effect of light quality on the pro-/antioxidant balance, activity of photosystem II, and expression of light-dependent genes in eutrema salsugineum callus cells. Photosynth Res. 2018;136:199–214.
122. Qin Y, Zhang Y, Zhang S, Wu T. Induction of callus and establishment of cell suspension and effects on tea polyphenols in the cell suspension system of tea plants by PGRs. Sci Hort. 2023;310:111770.
123. Sun M, Zhu L, Zhang Y, Liu N, Zhang J, Li H, Shi L. Creation of new germplasm resources, development of SSR markers, and screening of monoterpene synthases in thyme. BMC Plant Biol. 2023;23(1):13.
124. Willson KG, Cox LE, Hart JL, Dey DC. Three-dimensional light structure of an upland Quercus stand post-tornado disturbance. J Forestry Res. 2020;31:141–53.
125. Zhao Z, Liu L, Li S, Hou X, Yang J. Advances in research on the relationship between thymoquinone and pancreatic cancer. Front Oncol. 2023;12:1092020.

Publisher's note